Uplift of the Central Andean Plateau and Bending of the Bolivian Orocline

BRYAN L. ISACKS

INSTOC Cornell Andes Project, Department of Geological Sciences, Cornell University, Ithaca, New York

The topography of the central Andes can be considered the primary tectonic "signal" of late Cenozoic mountain building in an arid region where the effects of uplift and magmatism are little obscured by denudation. The spatial coverage of the topographic signal is more complete than that for sparsely sampled geological and geophysical data. A color-coded image of digitized topography between 12°S and 37°S highlights the Altiplano-Puna, one of the world's most remarkable plateaus, and reveals important physiographic clues about the formation of that major feature. The topographic data combined with information on structure, magmatism, seismicity, and paleomagnetism support a simple kinematical model for the late Cenozoic evolution of the central Andes. The model does not require collisional effects or enormous volumes of intrusive additions to the crust but instead calls upon plausible amounts of crustal shortening and lithospheric thinning. The model interrelates Andean uplift, a changing geometry of the subducted Nazca plate, and a changing outline (in map view) of the leading edge of the South American plate. Crustal shortening has accommodated convergence between the Chilean-Peruvian forearc and the South American foreland. The Altiplano-Puna plateau can be constructed by a combination of crustal shortening and thickening and lithospheric thinning above a shallow dipping (20°–30°) subducted plate. The seawardly concave bend of western South America, the "Bolivian orocline," was enhanced but not completely produced by an along-strike variation in the amount of late Cenozoic shortening. Maximum shortening in Bolivia both produced the widest part of the plateau and increased the seaward concavity of the Bolivian orocline. The along-strike variations of shortening are hypothesized to result from corresponding along-strike variations in the width of a weakened zone in the overriding plate. Weakening occurs above the wedge of asthenosphere located between the subducted and overriding plates; hence the width of the zone of weakening depends upon the dip of the subducted plate. Two types of shortening are recognized: (1) a widespread, basin-and-range, Laramide-like shortening that characterizes modern activity in the Sierras Pampeanas and late Miocene deformation of the Altiplano-Puna and (2) on the eastern side of the cordilleras and plateau, an east verging foreland fold-thrust belt in which the underthrust foreland compresses and thickens the ductile lower crust and produces a plateau uplift of the upper crust. The second type of shortening can be applied to Plio-Quaternary deformations throughout the central Andes but with a substantial narrowing of the region of plateau uplift in Peru and south of 28°S. A proposed monoclinal flexure of the upper crust on the western side of the plateau uplift explains the remarkably simple and regular morphology of the main western slope of the central Andes. The monocline is located above the tip of the asthenospheric wedge between the converging plates; it is postulated to occur above the western limit of lower crustal thickening. In the regions of horizontal subduction the monocline can be associated with a late Miocene asthenospheric wedge tip.

INTRODUCTION

The Altiplano of southern Peru, Bolivia, and northern Chile and the Puna of northwestern Argentina together form one of the world's great plateaus. Average elevations near 4 km occur over an area about 300 km wide and 2000 km long. Although the plateau seems clearly associated with the subduction of the Nazca plate beneath western South America, its origin remains controversial. While many studies have assumed that modern Andean topography is due to crustal thickening produced by magmatic additions of material from the mantle [e.g., *Thorpe et al.*, 1981], an increasing amount of evidence points to the importance of compressional crustal shortening in the formation the modern central Andes [e.g., *Dalmayrac et al.*, 1980; *Burchfiel et al.*, 1981; *Jordan et al.*, 1983a; *Chinn and Isacks*, 1983; *Allmendinger et al.*, 1983 ; *Suárez et al.*, 1983; *Mégard*, 1984; *Lyon-Caen et al.*, 1985; *Sheffels et al.*, 1986].

In this paper I explore the hypothesis that Andean topography is largely a result of crustal thickening produced by structural shortening of the crust and of uplift due to thermal thinning of the lithosphere. I use topographic data in combination with published evidence about uplift and crustal deformation to support a model for the late Cenozoic evolution of the central Andes. The model connects along-strike changes in the amount of shortening in the upper plate with the shape of the subducted Nazca plate and with changes in the map view outline of the leading edge of the overriding continental plate. The key idea is that an along-strike variation in the amount of shortening implies the possibility of a change in the shape of the map view outline of the leading edge of the upper plate. If late Cenozoic shortening of the upper plate were to be a maximum in the region of the seawardly concave corner near the Peru-Chile border (near 18°S), then the map view curvature of the forearc must have increased. This provides a simple mechanism for the development of *Carey's* [1958] "Bolivian Orocline," a concept that has recently received support from paleomagnetic studies [e.g., *Kono et al.*, 1985]. The orocline can be viewed as a bending of a narrow forearc strip that is accommodated by a variable amount of shortening in a mobile belt between the forearc and the cratonic foreland.

The starting point of the model is the assumption that thermal weakening is caused by convective and magmatic processes in the wedge of asthenosphere located between the upper and subducted plates. Late Cenozoic magmatism, rather than supplying the large volume of crustal material needed to support the elevated terrain, can be taken as a sign of the process of thermal weakening that allowed the compressional failure of the overriding South American plate to happen. The along-strike variation in

shortening results from variations in the horizontal width of the zone of thermal weakening in the overriding continental plate. Since the width of the wedge of asthenosphere is determined by the dip of the subducted plate, the along-strike variation in shortening is thereby related to the geometry of the subducted plate. Although oversimplified and only kinematic, the proposed model is an evolutionary, three-dimensional one. Its success emphasizes the futility of trying to understand the subduction process with traditional steady state, two-dimensional cross-sectional models.

In the arid and largely unglaciated central Andes where denudation is minimized and the tectonic processes are youthful and ongoing, the topography is a direct, first-order expression of the endogenetic processes forming the mountain belt. Early work such as Bowman [1909a, b, 1916] clearly recognized the youthfulness of central Andean uplift and its plateaulike character. However, regional physiography has received very little attention in the dominantly geochemical, structural and geophysical approaches that characterize most modern study of the region (Coney [1971] is an outstanding exception). I present here a new view of the central Andean physiography based on digitization of 1:1,000,000-scale topographic maps now available for most of the region. The computer-generated color image of this digital data set is shown in Plate 1. The image depicts the regional-scale physiography in a particularly clear and accurate fashion. It preserves the detail lost in a similarly scaled conventional map in which topography would be shown by only a limited set of subjectively smoothed contour lines.

I first summarize relevant information about the plateau, then describe a two-dimensional model for shortening, and finally describe a three-dimensional model for the late Cenozoic kinematical development of the central Andean subduction zone and mountain belt. The digital topographic data support the models qualitatively by highlighting important physiographic clues to the nature of the plateau and by showing the very close spatial relationships of the plateau morphology to the structure of the subduction zone. In addition, the topographic data are used quantitatively to constrain models of along-strike variations in crustal shortening and thermal uplift. Additional sources of information include published studies of geology, seismicity, and gravity and the now extensive examinations that I have made of Landsat Thematic Mapper (TM) false color images of much of the central Andes. The analysis of TM data is ongoing and will be reported in subsequent papers but is mentioned in this paper in several instances where particularly clear support exists for aspects of the proposed model.

It is important to emphasize that this paper focuses only on the late Cenozoic development of the Andes with a model of deformation that adds incrementally to the integrated effects of previous Andean orogenic episodes that began in the Jurassic. It is widely recognized, however, that the Oligocene was a period of relative tectonic and magmatic quiescence and of probable reduction of relief formed in earlier Tertiary times. The Mesozoic and early Tertiary intrusives that are now found west of the modern Andes were presumably formed in a region of crustal thickening and uplift but are now located in an area of relatively low elevation and relief. Although the amount of crustal thickening remaining from these earlier deformational episodes is unknown, it is likely that a large fraction of the modern relief and crustal thickness did in fact form during the Neogene. As a first approximation, I ignore the effects of pre-Neogene deformation.

THE ALTIPLANO-PUNA PLATEAU

The Plateau

As shown in Plate 1 and Figure 1, a single broad plateau is the main continental-scale feature of the central Andes between about 15°S and 27°S. North and south of the plateau the mountain system narrows considerably but continues with average elevations greater than 3 km along the high Andean cordilleras of Peru and along the Chile-Argentine border (between 27°S and about 34°S). For convenience, I distinguish these two segments of the Andean mountain system located northwest and south of the plateau as the "Peruvian segment" (5°–15°S) and the "Pampean segment" (27°–34°S), respectively.

The hypsometric curve for the plateau (Figure 2) has a sharp break in slope at an elevation of 3.65 km, approximately the elevation of the extensive and internally drained basins of the Altiplano and Puna. Much of the remaining area of the plateau is characterized by moderate relief with elevations in the range of about 3.5–4.7 km. As recognized by Bowman [1909b] many years ago, peneplanation is the dominating fact in the physiography of the region. The other dominating factor is the pervasive volcanism. Many of the highest peaks are volcanic constructional landforms, although areas of high structural relief are also found along the eastern edges of the northern and southern parts of the plateau.

The extrusive material largely sits on top of the plateau rather than forming the volume of the plateau itself. The upper Miocene–Recent extrusives form only a thin cover on a surface of beveled older structures, as is clearly shown by the studies of Baker and Francis [1978] and Baker [1981], by numerous detailed reports of the areal geology of specific regions of the plateau, and quite clearly by Landsat TM imagery that I have examined for much of the plateau. Large areas are covered by only a thin layer of extrusives, while the high stratovolcanos, although quite numerous, contribute relatively little to the total volume of elevated terrain. In detailed studies of two particular areas of the southern Altiplano of Bolivia and Chile that are largely covered by upper Miocene to Recent volcanic rocks, Baker and Francis [1978] and Kussmaul et al. [1977] estimate volumes that amount to an average thickness of extrusives of only about 0.3 km. With the digital elevation data and the assumption that elevations above the plateau level of 3.65 km all represent extrusives, an average thickness of 0.5 km is obtained for the entire area of the plateau. This estimate is probably too high since some of the highland area of the plateau is not volcanic.

The plateau includes a large area of internal drainage outlined by the watersheds shown in Figure 1. The internally drained region includes the large Altiplano basin of southern Peru and Bolivia and the more fragmented basins of the Argentine Puna and the Chilean Altiplano and Salar de Atacama. In many of the basins, compressionally deformed upper Tertiary strata are exposed, and the bounding highlands were uplifted by basinward verging thrust faulting [e.g., Turner, 1960, 1961; Schwab, 1970; Evernden et al., 1977; Martinez, 1980; Jordan et al., 1983a; and Jordan and Alonso, 1987]. Much of the characteristic basin and range morphology of the Argentine Puna is a manifestion of this type of compressional deformation, as is the the area around Lake Titicaca [Newell, 1949; Martinez, 1980]. The unconformity between the generally flat and little deformed uppermost Miocene–Recent extrusives and the older folded and reverse-faulted strata is seen throughout the plateau and gives evidence
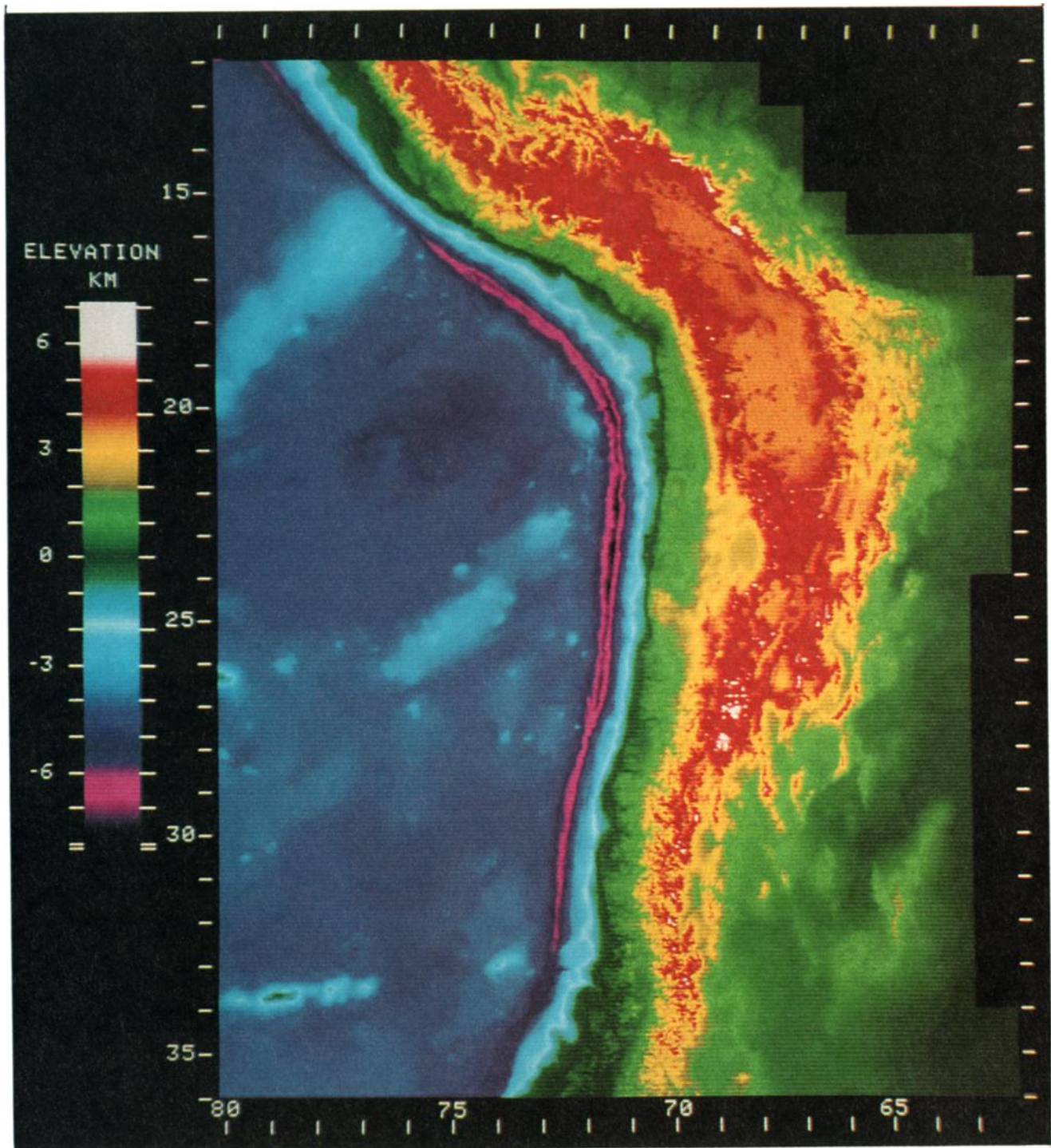
Plate 1. Computer display of digitized topography of western South America. Subaerial data are digitized as point elevations on a grid spacing of 0.05° of latitude and longitude. The data are mainly from 1:1,000,000-scale Aeronautical Charts published by the U.S. Defense Mapping Agency; a few small areas missing from those charts are filled in using available Bolivian and Peruvian topographic maps. An offshore strip from the coastline to the outer slope of the Peru-Chile trench was digitized with the same grid spacing as the land data from the 1:1,000,000-scale bathymetric charts of Prince et al. [1980]. Remaining oceanic areas west of the Prince et al. map were taken from the NOAA SYNBAPS digital bathymetry file, resampled, and then "spliced" to the continental and trench data with International Imaging Systems model 575 image processing software. Each elevation sample is displayed as a pixel colored according to the scale shown on the left-hand side. No spatial averaging or smoothing was employed.
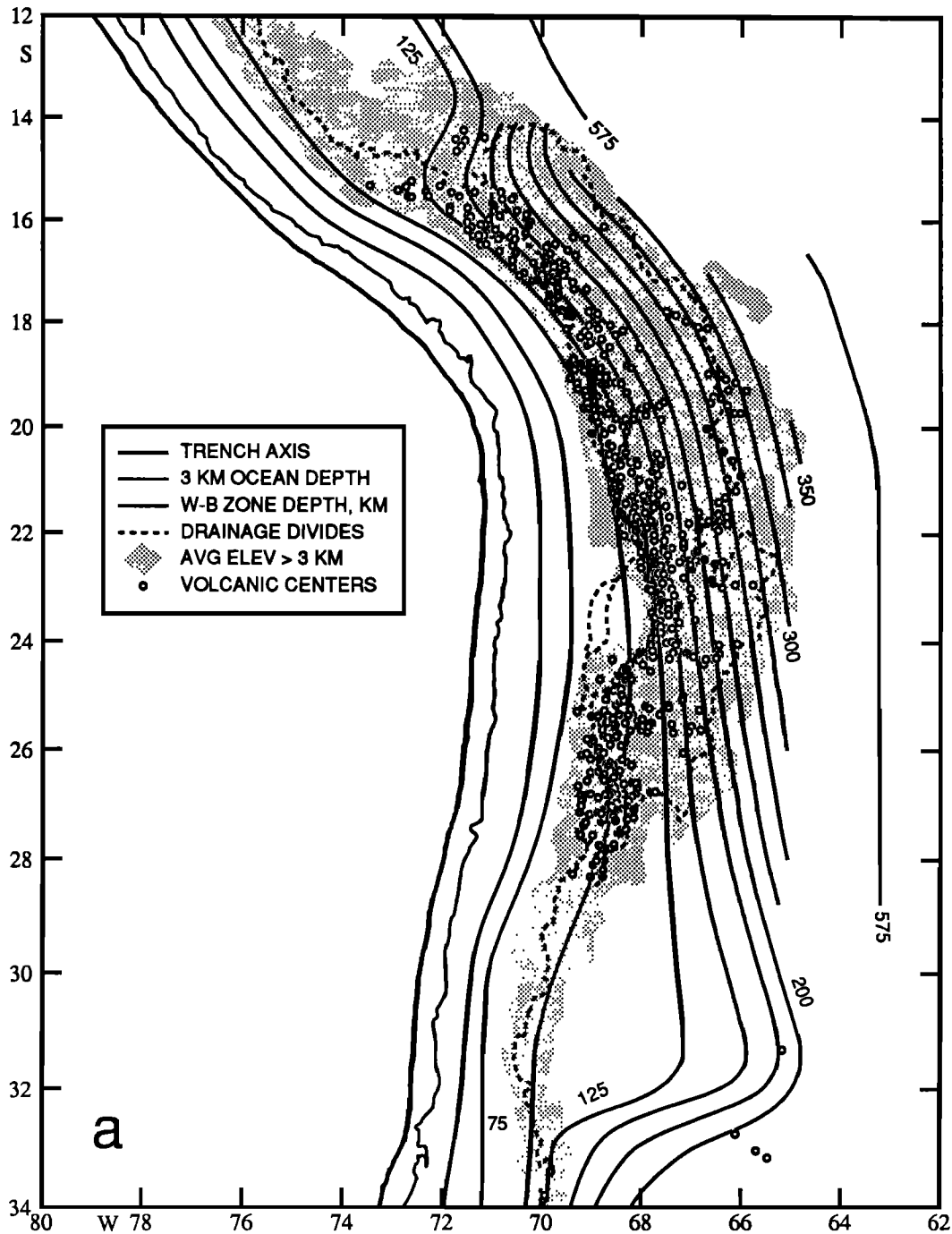
Fig. 1. (a) The shape of the subducted Nazca plate, volcanic centers, drainage divides, areas with average elevations above 3 km, and the axis of the Peru-Chile Trench. The contours of depth to the central part of the Wadati-Benioff seismic zone depict the shape of the subducted plate (T. Cahill and B. L. Isacks, unpublished manuscript, 1987). The Neogene volcanic centers were identified on Landsat MSS black and white imagery at a scale of 1:1,000,000 and represent volcanos mainly younger than about 10 m.y. The drainage divides were traced and digitized from the 1:1,000,000-scale topographic charts used for the digital topography. In the shaded areas, average elevations are greater than 3 km, as averaged within a "square" moving window with dimensions 0.25° in latitude and longitude and a 0.25° step. The axis of the trench was traced and digitized from the 1:1,000,000-scale charts of Prince et al. [1980]. (b) The coast line, borders between countries, and certain geographic and tectonic provinces discussed in the text, together with elevations above 3 km and the trench axis taken from Figure 1a. "F-P CORD" indicates the Frontal and Principal Cordilleras located along the Chile-Argentina border, and "AB" is the Atacama Basin (Salar de Atacama) of Chile.

that the compressional deformations of much of the plateau occurred during late Miocene time. These deformations are approximately coeval with important compressional deformational phases of the main cordilleras in the adjacent Peruvian and

Pampean segments north and south of the plateau [e.g., Mégard, 1984; Jordan and Allmendinger, 1986]. Together, the late Miocene deformations are for convenience referred to here as the "Quechua" phase, although studies in different areas reveal
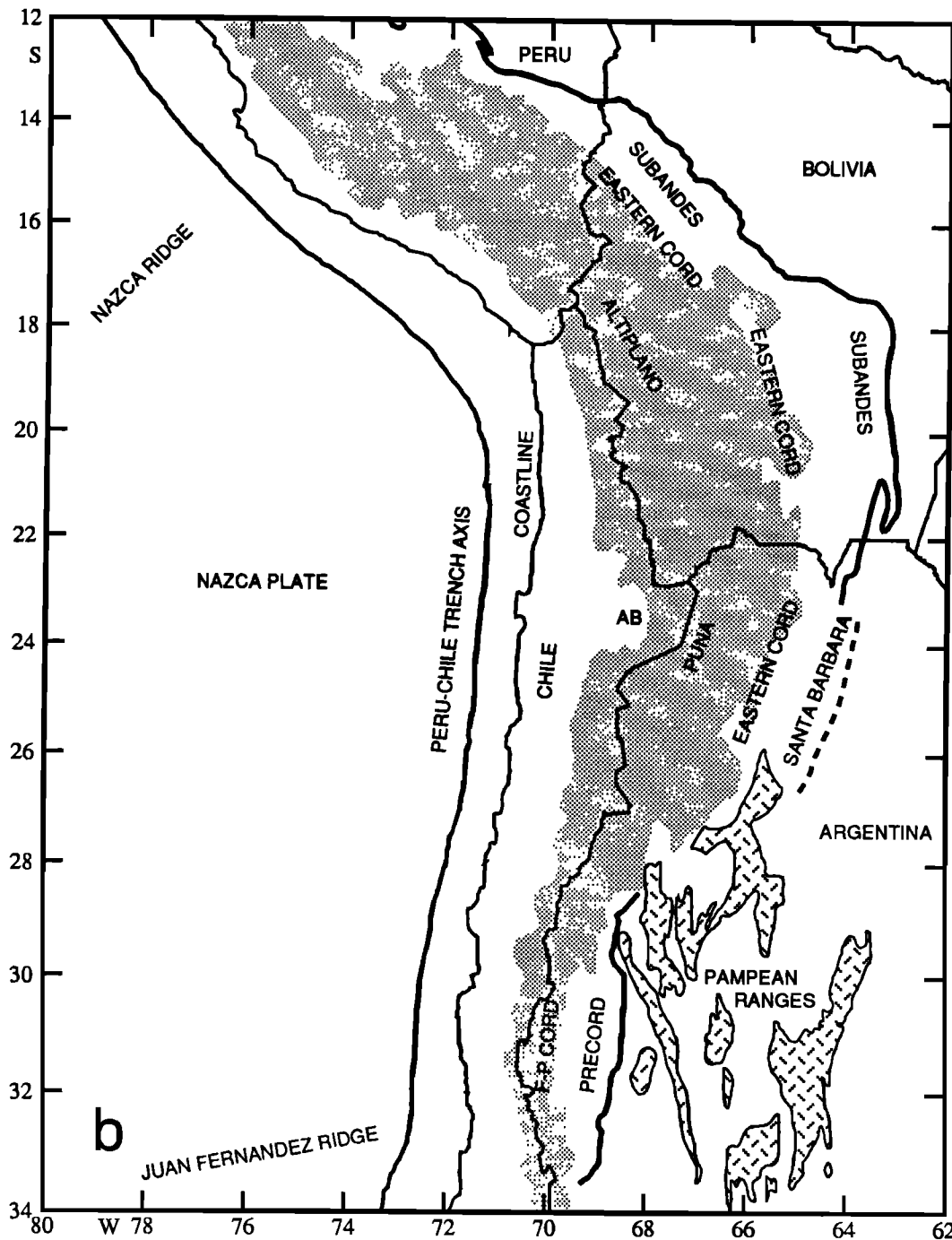
Fig. 1. (continued)

possibly significant regional variations in timing (e.g., compare *Jordan and Alonso* [1987] with *Mégard* [1984].

Except for the constructional volcanic edifices, much of the plateau now has a low to moderate relief. The reduction of structural relief that occurred during and following the Quechua deformations proceeded both by erosion of uplifted blocks and by filling of adjacent closed depressions, a kind of "cut and fill" process that tends to level the terrain in a situation where mass is not transported out of the internally drained system. This process created the numerous thick sections of late Cenozoic continental deposits that characterize much of the plateau [e.g., *Jordan and Alonso*, 1987]. The nonvolcanic areas of high relief are located

mainly along the eastern edges of the plateau where drainage removes material from the area and thereby accentuates relief. Notable areas of high relief that can be seen in Plate 1 are associated with the Mesozic and Cenozoic intrusions located along the northeastern side of the Altiplano and with basement involved thrust structures of the Eastern Cordillera located along the southeastern side of the Argentine Puna (see Figure 1).

Although some Pliocene–early Quaternary compressional deformation is documented for parts of the plateau, the main locus of the surface manifestation of post-Quechua compressional deformation appears to have shifted eastward to the eastern cordilleras and sub-Andean belts [*Turner*, 1966, 1969; *Martinez*,

1980; *Jordan and Alonso*, 1987]. An eastward shift also appears to have occurred in the adjacent Peruvian and Pampean segments [*Mégard*, 1984; *Jordan and Allmendinger*, 1986]. Late Quaternary extensional and strike-slip deformations developed within the plateau, at least in its southern and northern parts [*Lavenu*, 1978; *Sébrier et al.* 1985; *Strecker et al.* 1985; *Allmendinger*, 1986]. These youngest deformations appear to be small in magnitude compared to the compressional deformations, although *Green and Wernicke* [1986] claim otherwise for a part of the northern Altiplano of southern Peru.

The existence of a broad, internally drained area of low relief, now at elevations everywhere greater that 3.6 km, can be interpreted as an effect of youthful uplift, young enough that a 250–300 km width of elevated terrain has not yet been attacked by headward erosion from the flanking drainages. Although the drainage systems along the edges of the plateau operate over a nearly 3–4 km elevation differential, the rates of headward erosion may be small along much of the eastern and the western sides where the climates are quite arid. There are few constraints on the detailed chronology of uplift, but nearly all workers agree on a late Cenozoic time scale. A number of published studies report an acceleration in the late Miocene [e.g., *Segerstrom*, 1963; *Turner*, 1966; *Galli-Olivier*, 1967; *Rutland et al.*, 1965; *Hollingsworth and Rutland*, 1968; *Guest*, 1969; *Mortimer*, 1975; *Laubaucher*, 1978; *Martinez*, 1980; *Crough*, 1983; *Tosdal et al.*, 1984; *Jordan and Alonso*, 1987; *Allmendinger*, 1986; *Benjamin et al.*, 1987]. This timing would imply significant uplift during and after the pervasive Quechua deformations.

Eastern Thrust Belt

The eastern side of the plateau is formed by the major thrust belts of the eastern cordilleras and sub-Andean zones. These mainly Pliocene-Recent thrust zones can be traced along strike into the Peruvian and Pampean segments. In all three segments the eastern thrust belts are seismically active. In fact, it is now clear that crustal seismicity in the central Andes is concentrated within the eastern thrust belts and that the Altiplano-Puna regions are relatively aseismic [*Chinn and Isacks*, 1983; *Suaréz et al.*, 1983; *Froidevaux and Isacks*, 1984]. This result is in accord with the studies mentioned in the previous section that conclude that shallow crustal deformation has also become concentrated in the eastern thrust belts.

Several estimates of the amounts of shortening in the thrust belts are now available. *Allmendinger et al.* [1983] report at least 60 km of shortening based on a palinspastic reconstruction of *Mingramm et al.*'s [1979] section through the sub-Andean fold-thrust belt near 22°S. *Sheffels et al.* [1986] find 25–36 % shortening of the fold-thrust belt near 18°S where the belt is widest. This yields shortening values of about 150–225 km. For the same region, *Lyon-Caen et al.* [1985] estimate shortening amounts based on analysis of gravity data greater than 100 km and mention possible values as high as 400 km. *Jordan and Allmendinger* [1986] estimate 10–20 km shortening across the Pampean province of western Argentina near 30°–31°S which, when added to about 50 km shortening across the Precordillera fold-thrust belt [*Fielding and Jordan*, 1987; Allmendinger, personal communication, 1987], yields about 70 km for a section across the Pampean segment.

None of these estimates is tightly constrained, and none include the older Quechua deformations located west of the thrust belts. *Mégard* [1984] estimates 115 km for a part of the Peruvian segment that does attempt to include all late Cenozoic deformation. *Ramos* [1985] estimates about 30 km of Quechua shortening in the main cordillera at about 33°S in the southern part
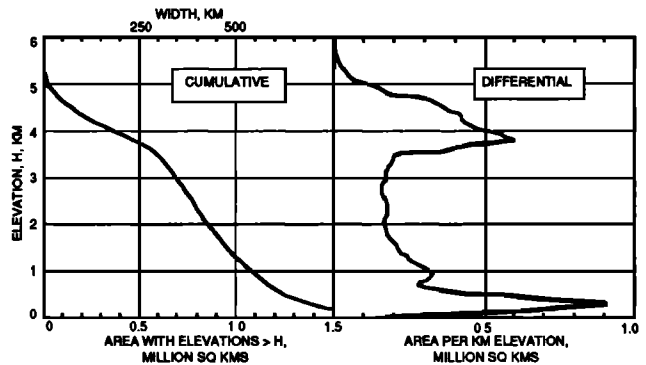

Fig. 2. Cumulative and differential hypsometric curves for the digitized elevations shown in Plate 1 for the region between latitudes 13°S and 29°S, the region of the Altiplano-Puna plateau. In the left-hand plot the variable plotted on the horizontal axis is the plan view area of land surface at elevations greater than the elevation plotted on the vertical axis. The horizontal scale at the top of the figure shows the effective "width" of a rectangular representation of the plateau as discussed in the text. In the right-hand plot the variable plotted on the horizontal axis is the plan view area of land surface per unit elevation taken as a function of elevation plotted along the vertical axis; the curve was computed as area per 0.03 km and normalized to area per 1 km.

of the Pampean segment; if added to *Jordan and Allmendinger's* [1986] estimates, this would produce a net shortening of about 100 km for the Pampean segment. Although sparsely distributed, these estimates of shortening all give strong support for large amounts of late Cenozoic shortening in the central Andes of the order of 100 km and more, amounts that must be accounted for in models of crustal thickening.

Along the eastern side of much of the Altiplano-Puna plateau the thrust systems verge eastward with the plateau overthrusting the foreland. In those regions the east facing topographic slope appears to coincide with the thrust belt. Although the western drainage divide is largely maintained by the volcanic constructions that build up and "dam" the western edge of the plateau, it is only in limited areas along the eastern watershed (such as the Frailes ignimbrite field near latitudes 19°S–20°S) that extrusives appear to exercise control on the position of the eastern drainage divide. Hence for much of the eastern side of the plateau the divide may be controlled by uplift of the hanging wall of the thrust system. In the cross section near 22°S published by *Allmendinger et al.* [1983] the high eastern edge of the plateau is located above the inferred position of the footwall ramp where the décollement ramps down to deeper levels of the crust. This result implies a direct relationship of the thrusting and topography. The inferred ramping of the décollement beneath the plateau implies that the shortening manifested in the eastern thrust belt is likely to be absorbed at depth beneath the main plateau uplift. I will use this concept in the proposed model of shortening.

South of about 22°S the eastern margin of the plateau is increasingly complicated by the appearance of structures characteristic of the Pampean segment, that is, by thick-skinned deformations with both east and west vergence that are found in the Santa Barbara system, the Argentine Cordillera Oriental, and the northern Sierras Pampeanas (Figure 1b). The morphology of the plateau edge becomes more irregular (Plate 1) and is characterized by large relief associated with Pampean-style, reverse faulted basement blocks. *Allmendinger* [1986] shows that the foreland-verging thrust system that bounds the southeastern margin of the Puna consists of short en echelon thrust segments which together accommodate shortening amounts of only tens of kilometers. The shortening accommodated by the other major structures in this complex region is unknown.

Still farther south in the Pampean segment itself, the Precordillera, a thin-skinned fold-thrust belt, forms the eastern slope of the main cordillera (the Cordilleras Frontal and Principal; see Figure 1b). In Peru a similar relationship exists between the Cordillera Oriental and sub-Andean zones with respect to the Peruvian "Puna" and Western Cordillera. In both the Pampean and Peruvian segments, décollements beneath the eastern fold-thrust belts are inferred to ramp down to the west into the crust beneath the eastern parts of the high central cordilleras [Mégard, 1984; Jordan and Allmendinger, 1986]. As proposed for the central plateau segment, the eastern thrust belts in the Pampean and Peruvian segments are also likely to be the surface expressions of shortening that is accommodated at depth beneath the main cordilleran uplifts. An added element in the Pampean segment is the significant amount of distributed foreland deformation east of, and probably beneath, part of the Precordilleran fold-thrust belt [Fielding and Jordan, 1987].

Western Monocline

As shown by the unsmoothed digital terrain model of Plate 1, the western slope of the plateau is a strikingly regular feature that is continuously traceable north and south along the flanking Peruvian and Pampean segments. The smooth morphology of the western slope contrasts with the complex and variable morphology of the thrust belts along the eastern side of the plateau. Although extrusives build up, spill over, and thus cover large areas of the western plateau edge, there are "windows" where an underlying subvolcanic basement can be seen. In these windows the edge and slope is formed by deformed pre-Neogene rocks that have been beveled to a relatively smooth surface, a surface that is now tilted to form the great western slope Andes. Much of the slope is covered by a thin layer of extrusives and by erosional debris forming a giant alluvial drape. These features can be clearly seen on Landsat TM imagery and on Chilean regional geological maps and have led several investigators to suggest that the uplift of the plateau was accommodated by a tilting or flexure of the crust [e.g., Muñoz, 1956; Mortimer, 1973]. I carry this forward by proposing that the western edge of the plateau is simply a crustal-scale monocline.

Although evidence for late Miocene-Pliocene compressive or extensional deformations have been reported for some areas of the western slope [e.g., Thomas, 1970; Lahsen, 1982], the amount of late Cenozoic deformations associated with these structures appear too small and spatially discontinuous to explain the large elevation differential across the slope and the continuity and regularity of morphology along-strike. Important Cretaceous–early Tertiary deformations have been recognized along parts of the slope [e.g., Vicente et al., 1979]. Some of these structures may have been reactivated in the late Cenozoic, but most of the deformation occurred too long ago to be associated with the uplift that formed the modern plateau and cordilleras.

In contrast to the northern Chilean region, the western slope along the Pampean segment is considerably more incised by transverse drainage into the Pacific Ocean. This is due primarily to the southwardly increasing amount of precipitation falling on the western side of the Andes. Nevertheless, the clear along-strike continuity of the western slope (demonstrated in the color image of topography) suggests that the monoclinal flexure continues through the Pampean segment. The same argument applies to the Peruvian segment, where transverse drainage is also developed. Examination of TM images suggests that the northward development of the spectacular transverse canyons of northern

Chile and southern Peru may be related to an increasing amount of glaciation at high elevations in the Western Cordillera. I hypothesize that the monoclinal structure is a continuous feature through all three of the segments. Between latitudes 18°S and about 26°S along the central plateau segment, transverse drainage to the Pacific is virtually nonexistant [Mortimer, 1981]. Thus the western monoclinal edge of the Andes is there preserved and particularly clear.

Relation to Subducted Plate Geometry

Western slope and asthenospheric wedge. Plate 1 and Figure 2 demonstrate that the great western slope of the Andes very closely parallels the trench axis and the trend of the inner slope of the trench, that is, parallels the outline of the leading edge of the South American plate. Both features show distinct changes in trend near latitudes 17°S, 27°S, and 33°S coincident with boundaries between major segments of the central Andean subduction system. Along the central plateau segment the western edge of the zone of volcanic centers (Figure 1a), the volcanic "front," is aligned along the western plateau edge and tracks the main western slope except in the region of 23°–24°S where the slope bifurcates to form the Atacama Basin.

In a study of the geometry of the Chilean interplate boundary between about latitudes 20°S and 40°S, Kadinsky-Cade [1985] shows that the main western slope of the plateau (or of the high cordillera to the south of the plateau) is located approximately above the downdip end of the interplate boundary. This is supported by the parallelism of the slope and the contour of 75 km depth to the Wadati-Benioff zone shown in Figure 1a. The western slope would thus track the axis of the trench if the interplate boundary were to have both a constant dip and downdip width as functions of along-strike distance. The geometry of the Chilean interplate boundary does not appear to change appreciably north of at least 33°S.

However, a more revealing association may be between the location of the western slope and the tip of the wedge of mantle that exists between the inclined subducted plate and the horizontal overriding plate. The wedge is presumably asthenospheric material that is relatively hot and weak. The tip of the wedge will be located near or just downdip of the interplate boundary. Nearly all models of the generation of subduction-related magmatism involve interactions between subducted material with the mantle material in the wedge; thus the tip of the wedge probably controls the location of the magmatic "front." The shape of the wedge and the movement of the subducted plate determine a special convective system, as shown by many published theoretical studies. It is thus quite reasonable to suppose that convection in the wedge promotes major modifications of the upper plate in the form of magmatic intrusions, thermal thinning, and consequent mechanical weakening. I thus propose that the parallelism of the western topographic slope and the trench is a result of the fact that the western slope tracks the tip of the asthenospheric wedge.

In areas of nearly flat subduction, as in the Peruvian and Pampean segments, a wedge-shaped region of mantle is found far inland of the trench, nearly 800 km in each of the segments, where the subducted plate finally bends downward and develops a significant inclination. However, there is good evidence that in both segments the present subducted plate shape has evolved from a more steeply dipping, late Miocene geometry that probably existed during much of the development of the main cordilleras in the two segments. In both segments the western slopes are closely associated with the western fronts of the now extinct Mio-Pliocene

magmatic zones. Well developed magmatic arcs existed prior to about 7–10 m.y., indicating that asthenospheric wedges existed beneath the cordilleras then. The near extinction of the magmatism in late Miocene times is taken to date the flattening of the subducted plates in both segments [Noble and McKee, 1977; Coira et al., 1982; Jordan et al., 1983b; Jordan and Gardeweg, 1987; Kay et al., 1987]. I thus hypothesize that in both the Peruvian and Pampean segments the main cordilleras were located over late Miocene asthenospheric wedges and that the western topographic slopes mark the tips of those previous wedges.

In fact, the topographic slopes are both now located where the subducted plates bend back from the 20°–30° inclinations of the plate boundaries to more nearly horizontal inclinations. The geometry of the plate boundary itself is quite similar throughout the three segments, and it is only below depths of about 75–100 km that the striking variations in dip of the subducted plate develop. If in the regions of horizontal subduction the subducted plate were straightened out to maintain the nearly 30° dip of the interplate boundary, the wedge tips so defined would track the western slopes.

Along-strike limits of the plateau. As shown in Plate 1 and Figure 1, the along-strike extent of the plateau coincides with the active Plio-Quaternary magmatic arc. In southern Peru the northern limits of the plateau and volcanic arc quite closely coincide with the sharp flexure (near 15°S) between the steeply dipping and nearly horizontal segments of the subducted plate. The flexure is developed downdip of the region where the map view shape of the leading edge of the overriding plate has a change in seaward curvature from convex (Peru) to concave (southern Peru-northern Chile). The strike of the flexure is approximately aligned along the direction of relative motion between the converging plates [Bevis and Isacks, 1984; Grange et al., 1984]. These results suggests a close connection between the development of the flexure and the shape of the overriding plate in map view.

However, the correlation of plateau and subducted plate geometry farther south is not as simple as indicated by Barazangi and Isacks [1976] or by Jordan et al. [1983a]. Near 27°S the high plateau narrows, and a single continental drainage divide replaces the two that delineate the Puna-Altiplano basin. Latitude 28°S is approximately the southern end of the zone of Plio-Quaternary magmatism. In contrast to these rather sharply defined southern boundaries of the plateau and magmatic arc, the Wadati-Benioff zone only gradually flattens between latitudes of about 21°S and 32.5°S [Bevis and Isacks, 1984; T. Cahill and B. L. Isacks, unpublished manuscript, 1987]. Significant flattening is already apparent at latitudes of 27°–28°S.

The development of the flattening between 21°S and 24°S is associated with a marked anomaly in the morphology of the western Andes in the region of the Atacama Basin. Outside of this region, topographic profiles from the trench axis across the forearc typically show a benchlike shape formed by two steeper parts, the inner trench wall and the main western slope of the plateau or high cordilleras, separated by a less steep part that includes the coastline. In the Atacama Basin region the western slope of the plateau bifurcates in map view, and a second bench (occupied by the Atacama Basin) is formed at an elevation intermediate between that of the coastal bench and the high plateau. The bifurcation actually begins near latitude 21°S to form the upper basin of the Loa River. The lower part of the western slope continues to parallel the trench axis, while the upper slope and magmatic arc follow a more nearly SSE trend that is parallel to the

trend of the intermediate depth Wadati-Benioff zone (compare Figure 1a and the topographic image). The upper slope and magmatic arc both swing back toward the trench near 24°S, and farther south, a single western slope again parallels the trench. The intermediate-depth contours (125 km and deeper) of the seismic zone do not swing back, however, but continue along a SSE trend and thus diverge from the shallow part of the plate boundary. This divergence produces a flat part of the subducted slab that progressively widens southward.

A clear implication of the southward flattening is that the curvature of the subducted plate downdip of the interplate boundary must change from convex upward where the plate dip continues to steepen with depth to concave upward where the plate bends back to nearly horizontal. This can be seen by comparing the sections in Figure 3 (see also Hasegawa and Sacks [1981]. Although the seismicity data still do not determine the exact location of the transition in curvature, it does appear to be south of the dogleg jog in the trend of the magmatic front near 24°S. The transition may well be located near the region of 27°–28° where there is a subtle but clear change in the trends of both the trench axis and of the western slope (see Plate 1 and Figure 2). The development of upward concave curvature of the subducted plate could thus be associated with the westward protrusion of the western topographic front that develops south of 27°S. This would place the transition adjacent to the narrowing of the plateau and near the southern end of the magmatic arc.

MODEL FOR PLATEAU UPLIFT

Altiplano section

As shown in the preceding section, a major feature of the central Andes is the east-west asymmetry of the mountain belt in terms of late Cenozoic structures and morphology: on the western side a monoclinelike crustal-scale flexure parallels the plate boundary, whereas a major thrust belt forms the eastern side. The shortening accommodated by the eastern thrust belt is roughly coeval with a plateaulike uplift of the Altiplano-Puna. The cross-sectional model shown in Figure 4 attempts to account for these features for a representative section through the Bolivian Altiplano (The model approximates a cross section in the region of 21–22°S).

In the first stage (Figure 4a) the upper plate is thinned during an episode of relatively low-angle (but not horizontal) subduction. The heating and thinning of the lithosphere may have started 25–30 m.y. ago, when widespread magmatism resumed after an Oligocene hiatus [e.g., Baker and Francis, 1978; Coira et al., 1982; Jordan and Gardeweg, 1987], and when the direction of plate convergence became more nearly normal to the plate boundary [Pilger, 1984; Cande, 1986; Pardo-Casas and Molnar, 1987].

The model starts with the assumption that processes in the wedge of asthenosphere located between the subducted and upper plates are effective in thinning the upper plate. Such processes may include convection in the wedge driven by the motion of the subducting plate, intrusion of magmas into the upper plate, and erosion of the lower part of the upper plate by lithospheric stoping or delamination. I hypothesize that these processes operate within a swath whose cross-sectional horizontal width is the distance between the wedge tip and the point at which the wedge reaches some specific vertical thickness. This thickness has to do with the as yet poorly understood convective processes in the wedge and can only be guessed. An estimate for the thickness of 250 km is
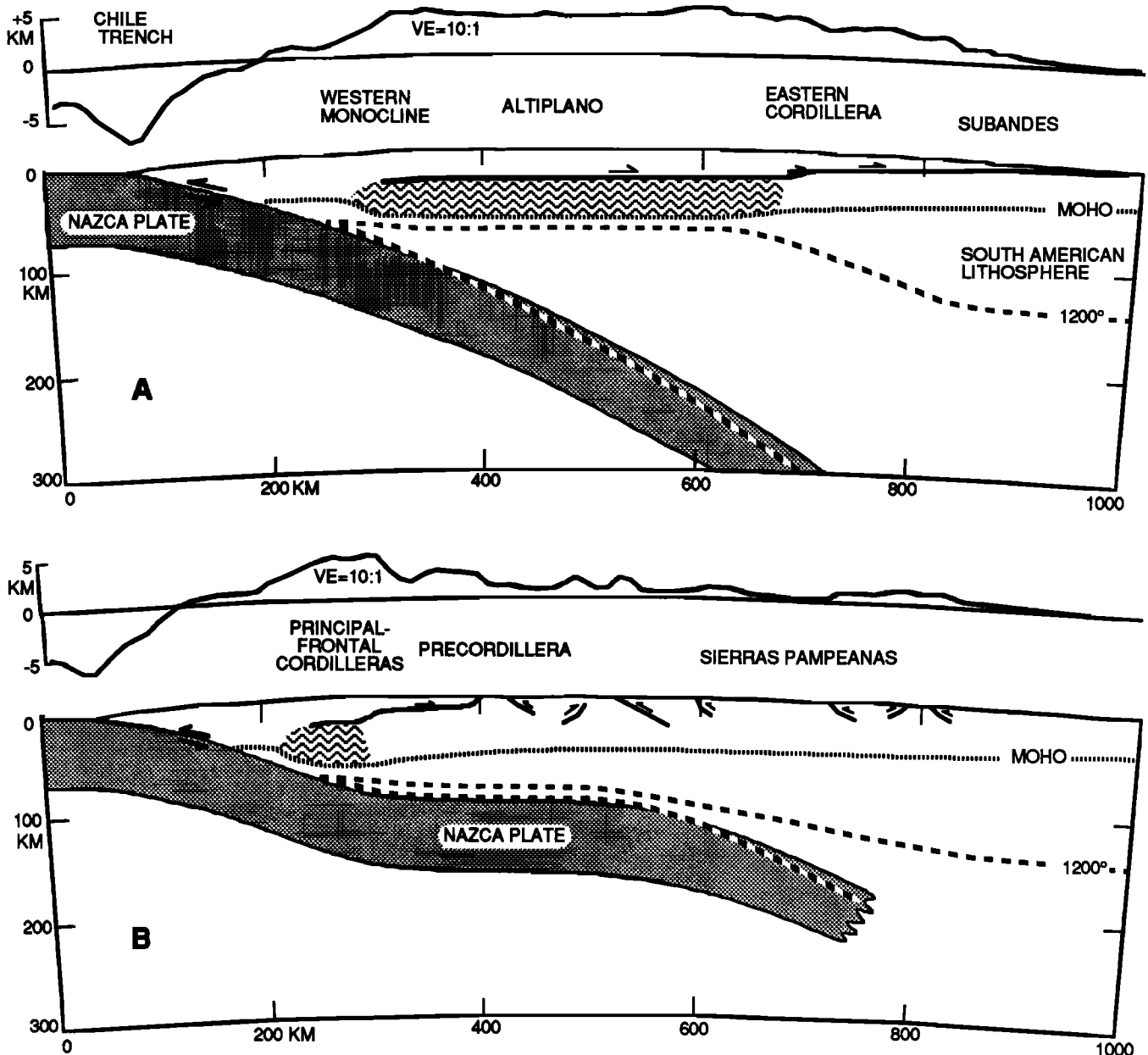
Fig. 3. Two cross sections showing topography and hypothesized deep structure. The upper section crosses the wide part of the central Altiplano, while the lower section crosses the Pampean flat slab segment. The western endpoints and the azimuths of the sections are 20.5°S, 72.0°W, and 083° for the upper section and 31.0°S, 72.0°W, and 090° for the lower one, respectively. Each topographic profile (upper plot in each section) shows digital elevations averaged along a swath 30 km perpendicular to, and 10 km along, the section. The plot has a vertical exaggeration of 10:1. The position of the subducted Nazca plate is fixed by the location of the Wadati-Benioff zone (T. Cahill and B. L. Isacks, unpublished manuscript, 1987). The wiggly line areas indicate shortened and thickened ductile lower crust. The upper crust overthrusts the foreland along a simplified single fault with motion indicated by the half arrow. Note the implied monoclinal structure of the upper crust forming the western topographic slope of the Andes. Other Pampean faults in the lower section are taken from Jordan and Allmendinger [1986]. The 1200°C isotherm indicates lithospheric thinning.

plausible in view of seismic studies of modern asthenospheric wedges [e.g., *Barazangi and Isacks*, 1971; *Utsu*, 1971; *Barazangi et al.*, 1975; *Hirahara and Mikumo*, 1980], but this choice remains a somewhat ad hoc starting point for the model.

With a fixed vertical thickness the horizontal width of the thermally affected swath will increase with decreasing angle of dip of the subducted plate. However, with a dip angle of zero, little or no asthenosphere would be located between the two plates. It is thus reasonable to suppose that as the dip decreases from vertical to horizontal in a plot of width of thermal effect versus angle of

dip, the width increases to a maximum and then decreases to zero as the dip approaches horizontal. A 20° dip is a plausible guess for the dip for maximum width; that is, at that dip angle there may still be enough volume in the asthenospheric wedge for the lithospheric thinning processes to operate. With a dip of 20° and the characteristic thickness of 250 km, the horizontal width of the wedge would be 500 km as shown in Figure 4a.

Magmatism, implying an efficient advective transfer of heat into the upper plate, would likely be associated with the thermal thinning of the lithosphere. Thus both volcanism and thermal
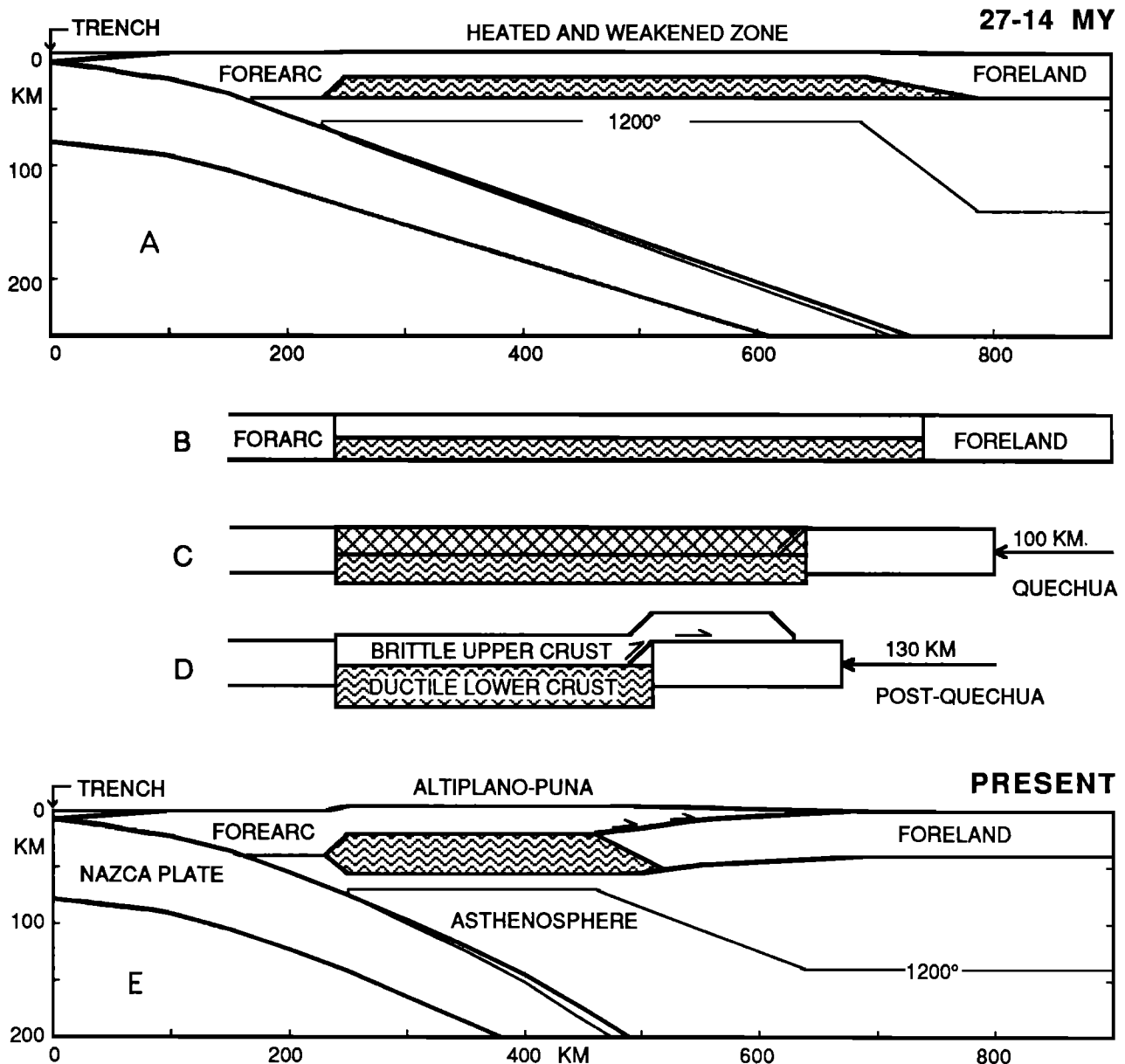
Fig. 4. Simplified model of late Cenozoic evolution of a section near 21°–22°S. Faults and ductile lower crust are shown as in Figure 3. The initial and final stages are depicted in the (a) upper and (a) lower sections, while the three middle sections show a very schematic (but balanced) block model of the crustal deformation. (b) is a simplified initial crustal section. (c) The cross hatching indicates pervasive shortening of the upper brittle crust during the "Quechua" phase of deformation. (d) For clarity the overthrusting of the upper crust onto the foreland is shown without any isostatic flexural adjustment; (e) the isostatic adjustment is shown.

uplift are implied in the early-middle Miocene phase depicted in Figure 4a, and both occur above a wide asthenospheric wedge. The thermal thinning would increase the temperature of the uppermost mantle and thus weaken that strongest part of the continental lithosphere. If the plate is subject to horizontal stress produced by the global convective system, the weakening would localize and concentrate deformation in the thermally affected zone and thus closely tie the spatial extent of the deformation to the position of the asthenospheric wedge.

I assume that the combination of global plate motions and mantle convection led to a situation where the continental plate overrides the oceanic plate and produces a pervasive compressional stress in the South American plate. The association of compressive stresses in the upper plate with relatively shallow

dipping subducted plates and the contrast between this mode of plate convergence and the one commonly found in the western Pacific, where the sinking of the oceanic plate "draws" the island arc seaward, are well recognized and are the subject of several papers [e.g., Wilson and Burke, 1972 ; Molnar and Atwater, 1978; Uyeda and Kanamori, 1979; Dewey, 1980]. The increased rates of convergence in late Miocene times may have helped trigger the failure [Pardo-Casas and Molnar, 1987].

The compressive failure of the weakened swath of lithosphere is postulated to have occurred in two phases. A widepread and pervasive horizontal shortening and vertical thickening of the crust (Figure 4c) corresponding to the Quechua phase of deformation was followed by a concentration of deformation along the eastern side of the orogen where the upper crust thrusted over the foreland

along an eastwardly verging thrust belt (Figure 4d). The latter phase produced the basic east-west asymmetry of the structure of the plateau and accounts for the evidence that the widespread Quechua deformation was followed by a concentration of compressive deformation along the eastern thrust belt.

In the latter phase, deformation of the brittle upper crust was concentrated along an eastern thrust belt, although the underthrusting foreland continued to compress the ductile lower crust west of the thrust belt. The consequent thickening of the lower crust produced a plateaulike uplift west of the thrust belt where the rising upper crust suffered little additional post-Quechua deformation. "Cut-and-fill" processes localized by the internal drainage system of the plateau reduced the relief of the Quechua structures on the uplifting plateau and thereby produced the characteristic physiography of the Altiplano-Puna. The concept for the second stage of compressive failure [Isacks, 1985] is similar (but independently derived) to that proposed by Zhao and Morgan [1985] for the uplift of the Tibetan Plateau. In the central Andes the "hydraulic ram" of Zhao and Morgan is the underthrusting South American foreland.

The model shown in Figure 4 implies that on the western side of the plateau a monoclinal flexure accommodates the differential uplift of the upper crust at the western limit of ductile thickening of the lower crust. The monoclinal flexure actually appears to form the western slope beneath the extrusive cover and is particularly well preserved in the hyper-arid desert of the central part of the plateau. The western limit of thickening of the lower crust is located at the western boundary of the heated and weakened zone in the upper plate, and this in turn is located above the tip of the asthenospheric wedge separating the converging plates. The position of the western topographic slope is thereby tied closely to the location of the magmatic front and the geometry of the subducted plate.

The model shown in Figure 4, although highly simplified, is scaled accurately to represent realistic amounts of crustal shortening and thickening with preservation of cross-sectional area; it is a "balanced" cross section. The plateau's present elevation is supported isostatically by a combination of crustal thickening and thermal expansion (or lithospheric thinning in the sense discussed by Turcotte and MacAdoo [1979]). Measurements of crustal thickness and densities in the region are still too crude to provide useful constraints on the details of the model. In the final stage (Figure 4e), a 4-km-high plateau is compensated by a thickening of the crust from 40 to 65 km and by a thermal thinning of the lithosphere from 140 to 70 km. This is a workable but nonunique model. If the shortening required to produce the thickening is averaged over 15 m.y., the convergence between the foreland and forearc would be about 1 cm/yr. This is a reasonable number for foreland fold-thrust belts [Allmendinger et al., 1985].

The model does not include additions of magmatic material from the mantle. As pointed out above, the volume of late Cenozoic extrusives contribute little to the overall volume of elevated crust. The intrusive volume is unknown, but Kay and Kay [1985] estimate a ratio of intrusive to extrusive volumes of about only 1:1 for the Aleutian island arc. Baker and Francis [1978] discuss ratios near 10:1 that would be required to build the Andes. This would lead to an extremely high rate of magmatic addition if the late Cenozoic time scale for the uplift is assumed [Isacks et al., 1986]. Baker and Francis, in fact, propose that intrusives have been thickening the crust since Jurassic times. This time scale, however, seems at odds with the considerable evidence mentioned in the preceding section that much of the uplift occurred in the late Cenozoic. In addition, the massive

Cretaceous and lower Tertiary plutons found in the coastal regions of Peru and Chile, the same batholiths that serve as models for crustal thickening by magmatic intrusion, are now located at low elevations and are not part of the present elevated mountain mass of the Andes. With the 100-150 m.y. time scale, it seems likely that erosional removal of mass would be able to keep up with the slow rate of addition of crustal material by magmatism.

As a first approximation, I therefore neglect the magmatic contribution, partly to see to what extent crustal shortening and lithospheric thinning alone can account for the plateau and partly because the intrusive volumes are quite uncertain. When information about crustal shortening, thickness, and density becomes sufficiently accurate to constrain models, then the discrepencies between observed and calculated parameters might be used to estimate the intrusive component.

Application to the Flat Slab Segments

The model for the uplift of the plateau shown in Figure 4 can also be applied to the adjacent along-strike segments of the convergent zone. The "plateau" between the monocline and thrust zone is taken to narrow into the high cordilleras of the two segments, becoming the Cordilleras Principal and Frontal in the Pampean segment and the Cordilleras Occidental and Oriental in the Peruvian segment. In fact, the Peruvian "Puna" [McLaughlin, 1924; Coney, 1971], a narrow high plateau region with mature relief characteristics similar to the Altiplano, is located between the Cordilleras Oriental and Occidental in Peru and is a northward continuation of the Altiplano. Coney showed a hypsometric curve for elevations within a small area of the central Peruvian Andes that is quite similar in form to that shown in Figure 2. The widths of the postulated shortened and thickened lower crusts beneath the cordilleran "plateaus" in the Peruvian and Pampean segments are smaller and involve less shortening for the same amount of uplift.

The wedges of asthenosphere hypothesized to be responsible for the weakening of the swaths are no longer located beneath the Peruvian or Pampean cordilleras, as already discussed, but are postulated to have migrated inland. The "flattening" of the subducted plate is partly the effect of the continental plate overriding the downward bend of the Nazca plate and thereby moving westward relative to the asthenospheric wedge. The tip of the wedge thus appears to move eastward or inland relative to the upper plate. The tip is now located at the eastern edges of the deformed forelands of the two flat slab regions and may be responsible for minor Neogene volcanism in these regions [Stewart, 1971; Kay et al., 1987].

In the middle Miocene before the overriding, a relatively narrow asthenospheric wedge is implied by the narrow late Miocene magmatic arcs in the Peruvian and Pampean segments. The narrow width of the wedge implies that the subducted plates then dipped more steeply beneath these segments than beneath the central Bolivian segment. This increased dip is supported by Kay et al. [1987]. The narrow thermally weakened swaths also failed under the pervasive compressional stress in the upper plate and thereby produced the crustal thickening beneath the high cordilleras of the two segments.

As the continental plate passed over the asthenospheric wedge in the Pampean segment, it was somewhat thinned and weakened, but the overridden and still nearly horizontal Nazca plate quickly replaced the lost continental lithosphere section to form a kind of double lithospheric structure. A thin, weak interface between the subducted and upper plates would still effectively couple the two plates in terms of vertical isostatic adjustment. The low regional

elevation of the Sierras Pampeanas east of the Precordillera (see Figure 3) could thus reflect the isostatic effect of the combined lithospheric thicknesses, while the deformations manifested by the Sierras Pampeanas could result from the decoupling of the thinned (and weakened) upper plate from the lower plate in respect to horizontal lithospheric stresses. The stress systems in the overriding plate and in the Nazca plate may be coupled mainly along the interplate boundary located west of the mountain belt and transmitted only through the upper plate. If the overriding plate is thinned, then the horizontal compressive stress is increased in the thinned section compared to the thicker craton to the east by the ratio of respective lithospheric thicknesses.

An alternative view is that the foreland deformations in regions of flat slab subduction are produced by the effect of shearing stresses accumulated along the large area of contact between the two plates [e.g., Dickinson and Snyder, 1978]. The problem with this hypothesis is that it does not explain why deformations do not extend east of the zone of plate contact where the accumulated stresses might be expected to be largest. It seems likely that shear heating within the plate boundary interface zone (located beneath the Chilean forearc) would reduce the strength of the zone downdip of the interplate boundary [e.g., Yuen et al., 1978]. This is supported by the apparent maximum depths of interplate earthquakes of about 60 km [e.g., Chinn and Isacks, 1983; Kadinsky-Cade, 1985] and the lack of evidence of giant interplate events that would involve seismogenic slippage along the nearly horizontal parts of the interface zone. Thus the coupling between the plates in terms of horizontal compressive stress may be concentrated in the forearc interplate boundary.

Bird [1984] argues that Laramide deformations of the western United States resulted from a shearing of the lower crust and lithosphere by the eastward moving, horizontal Farallon plate beneath western North America. The rotational shearing transported lower crustal material eastward and thereby thickened the foreland crust. The Pampean deformations are at an early stage compared to the duration of the the Laramide orogeny, so the effects of shearing of the lower Pampean crust would not yet be so large as in the Laramide case. The topographic profile shown in Figure 3 is still probably dominated by the effects of the Miocene episode of steep subduction and associated crustal shortening and thickening beneath the high cordilleras and Precordillera and by the isostatic effects of the overriden Nazca plate.

It is interesting that although foreland basement deformation of the Peruvian segment is reported [e.g., Suárez et al., 1983; Chinn and Isacks, 1983], these deformations appear quite reduced in extent and amount compared to the Pampean segment. This contrast suggests that flat subduction does not necessarily produce Laramidelike structures.

MODEL FOR THE BOLIVIAN OROCLINE

The terms "back arc" and "forearc" were originally introduced to describe western Pacific island arcs. Karig and Moore [1975] discuss the forearc as a deformable beam (in map view), and Karig et al. [1978] argue that the Marianas forearc deformed somewhat in accommodating the opening of the Marianas basin (see also McCabe [1984], and Faure and Lalavée [1987]. Although the concept of a narrow forearc platelet is most obvious when applied to western Pacific Island arcs with large amounts of back arc extension, it can also be usefully applied to South America. The Andean "forearc" is a long narrow plate located between the interplate plate boundary and the zone of "back arc"

deformation. In map view the boundaries of the forearc would be the axis of the trench and the western topographic slope. A movement of the forearc relative to the South American craton must be taken up in an intervening zone of deformation. The movement of the forearc could consist of a rotation of the forearc as a whole combined with a change in its map view shape. It is important to point out that because the forearc is very long and narrow, a rather substantial change in shape could occur with relatively little deformation in the forearc itself.

The spatial relationship between the present Andean forearc shape and the geometry of the subducted Nazca plate can be taken to suggest that the forearc did, in fact, change shape during the late Cenozoic. The divergence south of 22°S between the strikes of the subducted Nazca plate at depths greater than about 150 km and the modern plate boundary suggests that the shape of the deeper part of the subducted Nazca plate reflects an older plate boundary configuration that is less indented than the present one. Figure 1a shows that the plan view shape of the 150-km contour is distinctly less embayed than the trace of the modern trench axis. The implication is that the westward concavity of the forearc increased during the subduction of the seismically visible part of the Nazca plate, i.e., during the past 12 m.y. [Wortel, 1984; T. Cahill and B. L. Isacks, unpublished manuscript, 1987].

Along-strike variations in the amount of shortening in the zone of accommodation between the forearc and South American craton could imply a change of shape of the forearc. Since the Puna-Altiplano is located inland of the indentation of the Peru-Chile coastline, it is reasonable to suppose that the plateau and the indentation are related. In particular, the indentation could be produced, or at least enhanced, if the along-strike variation in shortening were a maximum in Bolivia adjacent to the indentation. The fact that this is where the Andes reach maximum width encourages this point of view.

Data to constrain the movement of the forearc relative to the craton include estimates of the amounts of shortening across the Andes at various latitudes and paleomagnetic determinations of rotation of the forearc relative to stable South America. These two lines of evidence are developed in the following section. Direct structural evidence of deformations associated with bending of the forearc is so far generally lacking, but, as mentioned above, these deformations are likely to be small relative to those in the back arc that absorb the relative motion between the forearc and South American craton.

Along-Strike Variations of Cross-Sectional Area

Area measurements. The amount of shortening is not accurately constrained in any single cross section through the central Andes, although rough estimates are available for several sections. I attempt to add to these estimates by considering the cross-sectional area of the uplifted terrain as an effect of crustal shortening and thickening. The digitized topography is easily used for this purpose.

The cross-sectional area is measured for each of the 22 profiles shown in Figure 5. The elevations are averaged within a moving window 100 km wide (perpendicular to the cross section) by 10 km long, and the resulting curve integrated to give the total cross-sectional area above a base level of 0.3 km. The base level is an estimate of the elevation of the plains east of the the Andes that are unaffected by the uplift. The areas so calculated are plotted against the along-strike position of the profiles as measured by distance along a line paralleling the trench axis but located 300 km to the east of it. The distance of 300 km is measured from the
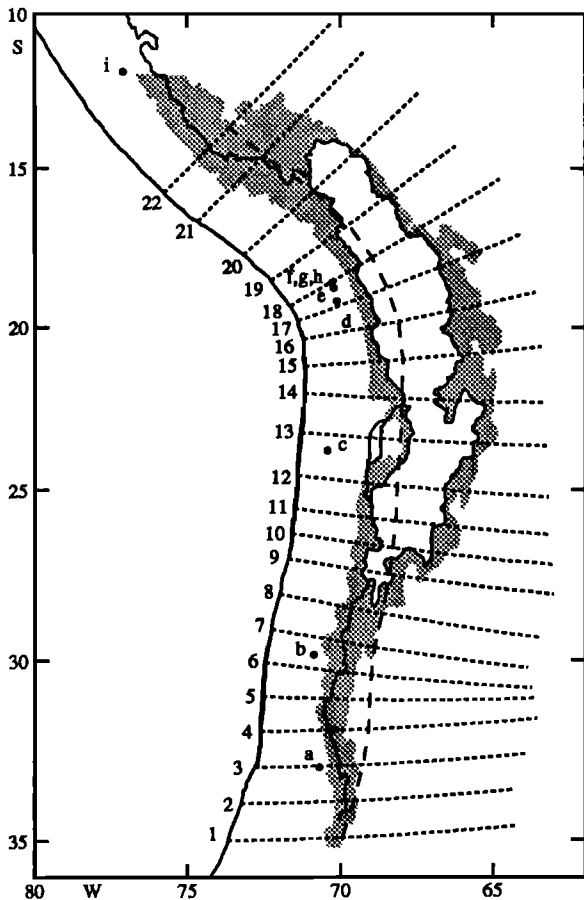
Fig. 5. Map showing 22 cross sections along which the cross-sectional area measurements plotted in Figure 6 are determined. The dashed line is located 300 km from trench (measured along the section lines); the along-strike distance plotted in Figure 6 is measured from south to north along this line. The axis of the trench, areas with average elevations greater than 3 km, and drainage divides are taken from Figure 1. The map is extended to 10°S to show locations of paleomagnetic data plotted in Figure 6, although the digital topography and averaged elevations end at 12°S. The letters identifying the sites of paleomagnetic studies are referenced in Figure 6.

trench axis along each of the 22 section lines. This "strike" line passes through the main uplifted area and is used only as a convenient linear measure of along-strike distance within the mountain belt. The 22 great circle projection lines define a rough curvilinear coordinate system fixed to the curved shape of the orogen, with a second set of approximately orthogonal lines (parallel to strike) located at fixed distances along the section lines.

The calculated cross-sectional areas are plotted for each section in Figure 6. Comparison with Figure 5 shows that the area is a maximum for section 16 across the wide part of the Bolivian Altiplano and Eastern Cordillera. The maximum also coincides with the bend in the coastline near the Peru-Chile border. This result indicates a maximum of shortening where the forearc has moved farthest back toward the craton, in agreement with the hypothesis of oroclinal bending.

Model of shortening. I examine the orocline hypothesis with the very simple model illustrated in Figure 7. The 12 m.y. time interval shown in Figure 7 is chosen to include the primary phases of compressional deformation and uplift. The actual timing is not well constrained. Thermal uplift and weakening of the upper plate

probably began earlier when widespread magmatism started about 25–30 Ma.

The trench axis, digitized from the 1:1,000,000 bathymetric charts of *Prince et al.* [1980], is an easily definable and convenient delineation of the shape of the forearc. Although a line in the center of the forearc would be more accurate, I approximate the deformation of the forearc by the deformation of a line delineating its western border. A problem with this simplification is that accretion of sediments during the time period considered would be equivalent to a movement of the trench axis seaward relative to the craton. However, this effect is not likely to be appreciable except south of 33°S where large volumes of accreted sediment are present [*Schweller et al.*, 1981].

In developing the model the present geometry was taken backward in time. The present trench axis was first rotated eastward together with the South America plate according to *Chase* [1978]. Then, to model the Andean shortening, the axis was moved relative to the craton by a westward translation and map view deformation to (1) produce a trend south of 20°S that is more nearly parallel to the strike of the deeper parts of the Wadati-Benioff Zone (which would have been subducting near the surface then), and (2) produce shortening amounts that are in agreement with the available constraints. These constraints, discussed in a previous section, are chosen (with amounts added for shortening not calculated in the referenced studies) as follows: 90 km at latitude 31°S [*Jordan and Allmendinger*, 1986], 120 km near 22°S [*Allmendinger et al.*, 1983], 250 km near 18°S [*Lyon-Caen et al.*, 1985; *Sheffels et al.*, 1986], and 100 km in the Peruvian segment north of the Altiplano near 10°S [*Mégard*, 1984].

In Figure 7 the sequence described above is reversed to show a forward evolution in time since 12 Ma. The oceanic plate is held fixed relative to the WSW movement of the overriding South American plate. The hypothesized trench axis 12 m.y. ago is rigidly rotated with the South American plate and then translated and deformed eastward to its present shape. The two motions of the forearc are artificially separated in Figure 7 only to isolate the motion of the forearc relative to the craton and not to imply a sequential chronology.

The actual trajectories of the motions of points in the forearc relative to the craton are not known; one possibility is that the trajectories are more or less parallel to the direction of relative motions between the Nazca and South American plates, as shown in Figure 7. The motions can then be decomposed into two components, one perpendicular and one parallel to the local strike of the forearc. These motions are assumed to be taken up in the deforming belt east of the forearc by shortening and vertical thickening for the perpendicular component and by horizontal rotational shearing for the parallel component. The model of shortening shown by the shaded area in Figure 7a is calculated as the distance between the deformed and undeformed trench axes measured perpendicular to the local strike of the present trench axis. This is of course only a very rough first approximation to the heterogeneous, three-dimensional finite strain field within the upper plate.

The along-strike "location" of a calculation of shortening is pinned to the locations of the 22 sections shown in Figure 5 in the following way. The model shortening is measured at the intersections of the 22 section lines with the present trench axis. These positions are then projected along the section lines to the line located 300 km east of the trench axis, the "strike" line through the main mountain belt shown in Figure 5, to determine the appropriate along-strike distance corresponding to the calculated shortening. The values of shortening obtained in this
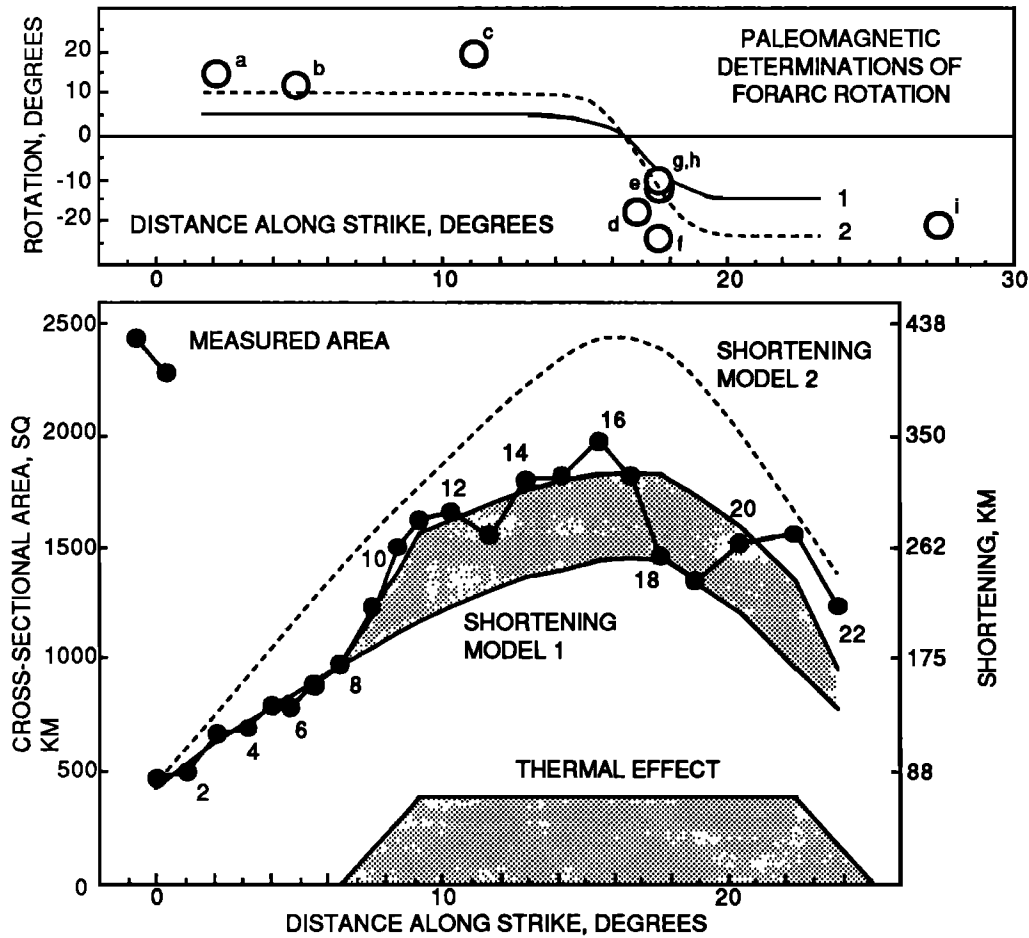
Fig. 6. The solid circles in the lower section show cross-sectional area measured along the numbered sections in Figure 5. The preferred shortening model 1 is shown together with another model 2. Model 2 has a maximum shortening of 425 km instead of 250 km. The combined shortening and thermal effect is shown only for the preferred model, and only model 1 is illustrated in Figure 7. The shortening values used in the models are given on the right-hand vertical axis. The upper panel plots paleomagnetically determined rotations of the forearc at the sites labeled by lowercase letters in Figure 5. In both panels the horizontal axis is distance measured along the dashed "strike" line in Figure 5. The paleomagnetic data include a, *Beck et al.* [1986]; b, *Palmer et al.* [1980a] and *Kono et al.* [1985]; c, *Turner et al.* [1984]; d, *Kono et al.* [1985]; e, *Heki et al.* [1985]; f, *Heki et al.* [1983] and Palmer et al. [1980b]; g, *Kono et al.* [1985]; h, *Heki et al.* [1985]; and i, *May and Butler* [1985]. The rotations corresponding to the two shortening models are shown by solid (model 1) and dashed lines (model 2) as indicated.

way are shown for model 1 on the right-hand ordinate of Figure 6.

Cross-sectional area calculated from shortening model. Shortening produces uplift by the isostatic effect of a thickened crust. Assuming preservation of two-dimensional cross-sectional area, then the sum of the cross-sectional area of elevated terrain and the depressed crustal root will equal the product of the original crustal thickness times the amount of shortening. An estimate of the elevation resulting from thermal expansion can be calculated for a given amount of lithospheric thinning and added to the effects of shortening. Magmatic additions are not included in this model. I also neglect the loss of material by erosion. In fact, for much of the central and southern parts of the plateau the erosional loss of material is probably quite minimal owing to the large areas of internal drainage and the aridity of the climate. The effects of extrusive additions and erosional losses can be considered as perturbations superimposed on the effects of shortening and heating.

The shortening model depicted in Figure 7 can be used to calculate the cross-sectional area of elevated material if the initial crustal thickness and crustal and mantle densities are assumed. I

use a simple Airy isostatic model with local compensation. Elevated material with density ρ_t is compensated by a root with density ρ_r and a mantle with density ρ_m. The initial crustal thickness is H_0, with an initial elevation h_0. After shortening, the sum of the additional elevation, $h - h_0$, and the added root r are integrated over the width affected by the shortening to give the added cross-sectional area of crust, A_c. If cross-sectional area is conserved,

$$A_c = S\,H_0$$

where S is the amount of shortening. The measured cross-sectional area of material elevated above the base level h_0 is A_r. With simple Airy isostasy we have

$$A_r = A_c \left(\frac{\alpha}{1+\alpha}\right) = S\,H_0 \left(\frac{\alpha}{1+\alpha}\right)$$

where

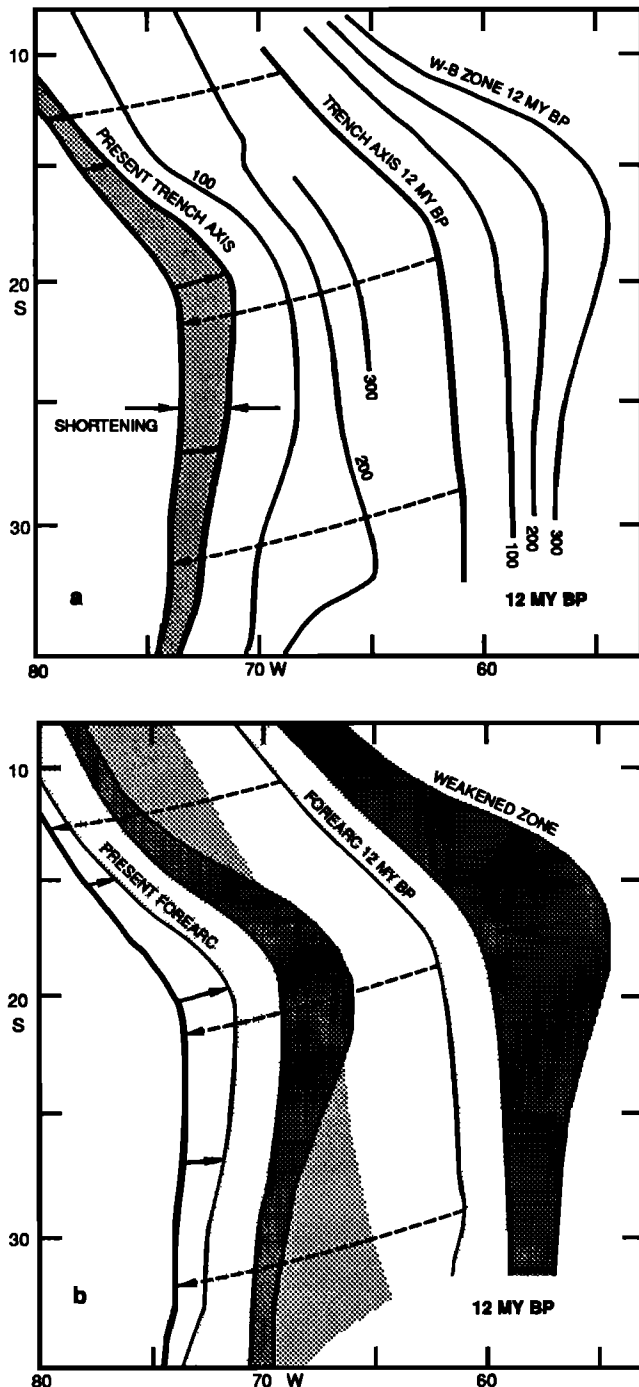$$\alpha = \frac{h - h_0}{r} = \frac{\rho_m - \rho_t}{\rho_t}$$

Fig. 7. Hypothesized evolution of (a) subducted plate and (b) upper plate since 12 Ma. The Nazca plate is held fixed with respect to the present map coordinate system while the South American plate and forearc are rotated. Figure 7a shows depths to the subducted plate in km for the present and for 12 Ma. For the same times, Figure 7b shows the hypothesized weakened zones (darkest shading) in the upper plate and the bending of the forearc. In Figure 7a the thick lines show the trench axis at 12 Ma, a rigid rotation of that axis for the 12 m.y. interval, and the present deformed axis. The shaded area between the last two positions of the trench axis represents the loss of surface area of the upper plate by the convergence of the foreland towards cratonic South America and is the basis for the preferred shortening model 1 shown in Figure 6. In Figure 7b the trench axis coincides with the western boundary of the foreland at 12 m.y. and at present, while the thick line is the 12-m.y. rigid rotation of the trench axis (before bending of the forearc) as also shown in Figure 7a. The trajectories of forearc movement toward the South American craton are abitrarily taken parallel to the directions of convergence of the two large plates. The lighter shading on the left side (present time) of Figure 7b shows areas of the upper plate weakened by passing over the asthenospheric wedge as the plate overrides the Nazca plate in the flat slab segments.

The cross-sectional areas determined from the shortening model can then be compared to the measured areas as in Figure 6 with assumed values for α and H_0. Wollard [1966] estimated an α of 1/7.5 based on empirical relationships between elevation and crustal thickness. For the crude model under consideration, we will use this value and assume an initial crustal thickness of 40 km. The values of shortening, S, are taken from the model shown in Figure 8A (the values are indicated on the right hand ordinate of Figure 7).

The resulting calculated curve mimics the main latitudinal variation of measured cross-sectional area, except that near 27°S the measured area ramps up to larger values. This occurs at the southern end of the Puna plateau. These higher values can be accounted for by a thermal effect, as discussed below. Another model with the shortening values increased in the Bolivian region relative to the flanks is also shown in Figure 6 (labeled model 2). The maximum shortening for this model is about 425 km. This is near the upper limit of the estimates of shortening discussed by Lyon-Caen et al. [1985]. This curve is everywhere above the measured shortening values, even without any thermal effects added. Model 1 seems to give a better fit, especially if thermal effects are added.

Thermal effect. I hypothesize that the excess elevation north of latitude 27°S for model 1 is mainly an effect of thermal expansion or lithospheric thinning. The thermal uplift for a 70-km thinning of the lithosphere is shown in Figure 6. This would correspond, for example, to a change of lithospheric thickness from 140 km, an arguable value for a stable continental lithosphere [Sclater et al., 1981], to 70 km. A simple linear approximation to a lithospheric conduction gradient is assumed [Turcotte and McAdoo, 1979] with a coefficient of thermal expansion equal to 3 x 10^{-5} cgs units.

An effective width of 400 km is then used to obtain the cross-sectional area that is produced by thinning of the lithosphere in the region of the Altiplano-Puna. The effective width is estimated on the basis of the hypsometric curve of Figure 2. This curve can be viewed as a kind of averaged, one-dimensional cross section. The abscissa is area of land above the altitude shown on the ordinate. If the plateau is simplified into a stack of rectangular prisms, the area shown is the product of the length of the plateau times a width within which elevations everwhere exceed the particular elevation. The length of the Puna-Altiplano region between about 13°S and 27°S, measured along strike, is about 2000 km. With this length fixed, the abscissa axis can then be labeled in terms of the width variable as shown along the upper part of Figure 2. The hypsometric curve shows that the averaged "side" of the plateau has a nearly linear slope between elevations of the plateau "edge" of 3.65 km and an elevation of about 1.3 km and an upward concave profile at lower elevations. I assume that the effective width is determined by a point halfway down along the linear part of the slope. The width of the plateau from this analysis is about 400 km.

The agreement of the estimated thermal effect and the magnitude of the discrepancy between observed area and area calculated from the shortening is quite good. Note that the along-strike extent of the thermal effect is simply fixed to produce the added area at 27°S. The interpretion of the 27°S jump in area is that north of this latitude the overriding and subducted plates are decoupled with enough intervening asthenosphere to permit thermal isostasy to operate, while to the south the nearly horizontal Nazca plate is coupled or "stuck" to the overriding plate and effectively holds it down. This transition in plate coupling is superimposed on a northwardly increasing amount of shortening to produce the observed northward increase in cross-sectional area.

The Quaternary magmatic arc ends near 28°S, just south of the southern end of the broad plateau, but there is no evidence of an abrupt change of dip of the subducted plate as found at the northern end of the plateau near 15°S. However, as suggested in a previous section, the curvature of the subducted plate just downdip of the plate boundary changes from convex to concave upwards near 27°S, and this change could be related to both the southward termination of magmatism and the isostatic coupling between the plates.

Effects of denudation. The erosional systems vary quite substantially around the edges of the Altiplano-Puna plateau. The western side is extremely arid with practically no streams reaching the Pacific between 18° and 26° [*Mortimer*, 1981]. In addition, the volcanism on the western edge of the plateau adds volume and acts against headward erosion by damming the plateau drainage. Aside from transfer of material down the giant alluvial drape along the western plateau slope, little volume has probably been removed from the western side of the plateau south of 18°S during the late Cenozoic phase of uplift. Headward erosion of Pacific drainage into the plateau has developed in the region north of 18°S as manifested by the spectacular series of transverse canyons in southern Peru. The still very youthful character of that physiography, however, suggests that the mass lost is small, that is, only that needed to fill the widely spaced canyons.

The eastern slopes are characterized by two regimes also separated approximately by the latitude 18°S, the Amazon River drainage to the north, and the semiarid Paraná River drainage to the south. Sections 18 and 19 cross into the Amazon system and show the largest deficiency in cross-sectional area with respect to the shortening model (Figure 6). I propose that this anomaly is, in fact, partly due to material removed by unusually high erosion rates in this region. Sections 18 and 19 cross into the drainage basin of the Beni River, a tributary of the Amazon River. Besides the vigorous erosion under modern conditions, significant glaciation of the Cordillera Real, the high massif forming the eastern edge of the Altiplano in the region crossed by sections 18 and 19, probably augmented the erosive efficiency of this drainage basin during the Pleistocene. The mountainous upper reaches of the Beni basin forms a deeply eroded segment of the eastern slope of the plateau, as is obvious from inspection of Plate 1. The physiography clearly suggests a large erosive cut into the side of the plateau. Filling this cut to the present level of the plateau would account for about half the discrepancy for sections 18 and 19.

In contrast, the drainage systems farther south are far less vigorous. In fact, the eastern drainage south of about 19°S actually carries little material to the Paraná River, since the rivers flowing out of the eastern Andes dry up within 100 km from the mountain front. This is associated with the increasing aridity south of 18°S and the decreasing amount of Pleistocene glaciation even at high elevations. The Andes between about latitudes 18°S and 33°S appear to be in a climatic belt [e.g., *Clapperton*, 1983] that is much less affected by the powerfully erosive alpine glaciations of the Quaternary that so profoundly affected the landscape of other segments of the mountain system.

The drainage system of the eastern slope of the plateau south of 18°S is incising the folded and faulted structures of the Bolivian Eastern Cordillera and sub-Andean thrust belts, but remnants of the high plateau surface are apparent in the topography and on Landsat imagery. For example, the Potosí intrusion, now exposed at elevations of 3 km (near 19.6°S, 65.7°W) is estimated to have been emplaced close to the late Miocene land surface with little material subsequently lost from above the intrusion [*Francis et al.*, 1983]. This contrasts with the Zongo intrusion located farther north in the upper reaches of the Beni River basin, where fission

track studies suggest removal of possibly more than 10 km of overburden during the past 10–15 m.y. [*Crough*, 1983; *Benjamin et al.*, 1987]. The loss of volume on the eastern slope south of 18°S may therefore be only the material missing from the youthful valleys and deposited in the foreland basin close to the eastern margin of the mountain front. The material in the foreland basins above elevations of 0.3 km is included in the cross-sectional area measurements. Thus it is reasonable to argue that significant effects of erosional removal of material are seen only in sections 18 and 19.

Why, then, do the deficiencies in cross-sectional area not extend to sections 20–22 as well, where the erosional vigor of the Amazonian drainage should perhaps be even greater than in sections 18 and 19? One problem is that the essentially two dimensional approach of the shortening models becomes increasingly inaccurate in the complex recurved northern end of the plateau. The sections taken there are somewhat oblique to the plateau and thus overestimate the cross-sectional area by an amount that accounts for about half of the discrepency between the observed and calculated areas.

Another possible effect is the erodability of the material. The batholiths of the eastern Andes of Bolivia and southern Peru become both more extensive and older from south to north [*Grant et al.*, 1979; *Dalmayrac et al.*, 1980]. In the Beni River basin the Triassic and late Oligocene–early Miocene plutonic bodies of the Cordillera Real form very high but areally small massifs within the surrounding weakly metamorphosed Paleozoic sedimentary rocks [e.g., *McBride et al.*, 1983]. The Beni River system has thus cut deeply into the less resistant rocks and has removed considerable material from the plateau. Farther north, the northeastern margin of the plateau is formed by areally extensive late Paleozoic and Mesozoic batholiths and associated strongly metamorphosed sedimentary rocks. These rocks may be have low rates of erosion compared to those farther south in the areas east of La Paz and thus, with their greater areal extent, may constitute a more effective bastion against the headward migration of the Amazonian drainage.

The relatively small anomaly near section 13 is associated with the Atacama basin, the steplike feature of the western side of the plateau discussed in a previous section. This anomaly does not appear to be explainable as an effect of denudation.

Paleomagnetic Data

Several investigators, notably *Kono et al.* [1985], argue that paleomagnetic data for the Chilean and Peruvian forearc support the hypothesis of oroclinal bending. *Beck et al.* [1986] point out possibly severe problems with the dating of remnant magnetizations and with the determinations of paleopole positions for cratonic South America (see also *Valencio et al.* [1983]) but nevertheless also show that the published data do seem to indicate a counterclockwise rotation of the coastal areas of Peru and northernmost Chile which contrasts with a clockwise rotation of the forearc farther south. This result is seen in the summary of selected forearc paleomagnetic data plotted in Figure 6.

Also shown in Figure 6 are simple geometric calculations of the rotations that occur in the models of deformation of the forearc relative to the craton. Again, the change in shape of the forearc is modeled by the change in shape of the trench axis. Both the model calculations and the selected paleomagnetic data are plotted with respect to along-strike positions determined by the 22 sections (Figure 5) as discussed in the previous section. The plot is extended northward to cover central Peruvian paleomagnetic determinations. The rotations calculated from the shortening model are done in a very crude fashion: the net rotations near

sections 4–12 and 20–21 are first determined, and the intervening curve is then roughed in with the assumed constraint that the change from clockwise to counterclockwise rotation occurs near sections 16–17 where the shortening reaches a maximum. More numerous and better constrained paleomagnetic data would justify a more sophisticated model of forearc bending and its associated rotations. At this stage, however, the fit of the data certainly encourages consideration of the oroclinal hypothesis. The magnitudes of rotation for model 1 tend to be too small, while model 2 provides a somewhat better fit. However, all of the paleomagnetic determinations shown are for Mesozoic magnetizations and thus integrate the deformation over the entire Cenozoic. Hence model 2 may be a better model for the entire Cenozoic, while model 1 is preferred for the Neogene.

In contrast, a complete straightening out of the Peru-Chile forearc, an effect discussed by *Kono et al.* [1985], requires rotations that are much larger than the well-determined rotations shown in Figure 6. This implies that the embayment of western South America was an inherited feature that was enhanced but not caused by Cenozoic shortening. I make use of this implication in discussing the late Cenozoic evolution of subducted plate geometry in the next section.

The blocklike clockwise rotation of Peru suggested by the paleomagnetic data as far north as 5°S [*Heki et al.*, 1983; *May and Butler*, 1985] implies a steadily decreasing amount of shortening toward the northwest within the Peruvian orogen. In agreement with this, results of a preliminary examination of the topographic maps of Peru north of 12°S show a clearly decreasing cross-sectional area toward the north. High altitudes still occur as sharp peaks in the glaciated cordilleras, but the total cross-sectional area decreases.

An apparent problem with the oroclinal hypothesis is the fact that the counterclockwise rotations characteristic of the Peruvian "block" are also found in the region just south of the Chile-Peru border (near 18°S) and therefore south of the presumed kink or hinge in the modern coastline where the rotations would reverse sign. However, the sharpness of the "kink" in the coastline near the Chile-Peru border is not a feature of the regional-scale morphology. The topographic image shows clearly that the coastline is not an accurate delineation of the more smoothly curved trend of the trench-mountain system but reflects a second-order structure on the topographic "bench" between the inner trench slope and the main western slope of the Andes. Thus in this region the shape of the coastline is an inaccurate indicator of the shape of the forearc. The model shown in Figure 7a for forearc bending has maximum curvature in the region of the Peru-Chile border, but the exact location of the change from counterclockwise rotation to clockwise rotation depends upon the detailed trajectories of material in the deforming forearc. The sites in northernmost Chile, in fact, appear to be slightly on the northern side of the maximum of inferred shortening, in agreement with the oroclinal hypothesis.

Relationship to a Changing Nazca Plate Geometry

Why should shortening vary along-strike? The following scenario is proposed with very tentative timing. During the period 25–12 Ma the map view outline of the leading edge of the overriding plate had a less pronounced (but still distinctly seawardly directed) concave curvature than now exists along western South America. During that period the subducted plate dipped at an angle of 20°–30° beneath the central part of the embayment but steepened to dips of 40°–60° in the adjacent

Peruvian and Pampean flanks. This geometry is schematically indicated in Figure 7a. A somewhat similar geometry can now be observed in the Izu-Bonin/North Honshu/Kurile system of the northwest Pacific. The Pacific plate dips gently (30°) beneath the North Honshu segment but steepens considerably in both the flanking segments, the Izu-Bonin and Kurile arcs. The overall form is that of a plunging anticline, a shape that can be topologically compatible with the concave shape of the trench axis in terms of deformations of an inextensible lithospheric shell [*Yamaoka and Fukao*, 1986, 1987].

In the central, shallow-dipping section the asthenospheric wedge was widest and consequently thinned and weakened the broadest swath of the upper plate, while a narrower magmatic and thermal system operated along the flanking regions where the subducted plate had steeper dips (see Figure 7b). At some time after the weakening began, the variable-width swath began to fail under the compressive stress system transmitted across the convergent boundary. A greater amount of shortening occurred in the central segment because the weakened area there was the widest. The assumption is that for a relatively constant lithospheric stress, shortening will proceed until a limiting elevation is reached [e.g., *Dalmayrac and Molnar*, 1981; *Suárez et al.*, 1983; *Froidevaux and Isacks*, 1984]; thus the amount of shortening will depend upon the width of the weakened swath.

The flanking segments of forearc consequently tended to override the oceanic plate relative to the central segment and thereby helped flatten the subducted slabs. However, the amount of movement of the flanking segments relative to the central segment is not enough to explain the flattening. An appeal must be made to other unconstrained factors. Possibilities include effects of subducted topography [e.g., *Kelleher and McCann*; 1976; *Pilger*, 1981; *Nur and Ben-Avraham*, 1981], subducted plate age [e.g., *Molnar and Atwater*, 1978; *Wortel*, 1984], relative and absolute plate velocities [e.g., *Luyendyk*, 1970; *Cross and Pilger*, 1982] and mantle flow [e.g., *Hager and O'Connell*, 1978; *Tovish et al.*, 1978].

The transition near 17°S in subducted slab dip is associated with the inflection of map view curvature of the trench axis and western slope. The sharpness of that inflection may have been enhanced by late Cenozoic crustal shortening, as suggested by the model of Figure 7. Thus the localization of the transverse flexure in the subducted plate may be partly a result of the late Cenozoic change in the outline of the leading edge of the overriding plate.

Quaternary Deformation of the Plateau

Evidence that extensional structures developed on the Altiplano-Puna plateau during the Quaternary can be related to the topographic effects of uplift as argued, for example, by *Froidevaux and Isacks* [1984]; (see also *Dalmayrac and Molnar* [1981], but the extensional structures have so far been reported only for the northern and southern parts of the plateau. According to the model of deformation shown in Figure 7, and assuming forearc trajectories relative to the foreland that are approximately parallel to the directions of motion between the foreland and the Nazca plate, shortening in the region of the northern Altiplano is oblique to the deformational zone with a significant component of left-lateral shearing along the strike of the orogen. This is consistent with the predominantly north-south direction of extension described by *Sébrier et al.* [1985] in the northern Altiplano. It is intriguing that the topographic image of Plate 1 shows rather marked linear features along the northwestern side of the Altiplano with northwest strike. Large yet unrecognized

strike-slip faults may exist in this region. The shortening in the southern part of the plateau is also oblique but with a right-lateral sense of shear parallel to strike. This is also consistent with the orientations of the young extensional and strike-slip deformations along the southeastern margin of the plateau reported by *Allmendinger* [1986].

The northern and southern "ends" of the plateau are, however, likely to be difficult to model, and field studies there are likely to reveal complex patterns of deformation [e.g., *Allmendinger*, 1986]. In those two regions the three-dimensional aspects of the deformation are important, preexisting structures control the details of the deformations [e.g., *Marocco*, 1978; *Allmendinger et al.*, 1983], and along-strike changes in thermal uplift are probably associated with the flattening of the subducted plates. Thus, for example, in the region of the southeast margin of the Argentine Puna, a northwardly increasing amount of shortening is accommodated by a northwardly changing style of deformation (in transition between the Laramide-style thick-skinned deformations of the Pampean segment and the Bolivian fold-thrust belt), and this is all overprinted by a thermal uplift that may now control the location of the southeastern plateau margin.

CONCLUSIONS

In this paper I have argued that the late Cenozoic uplift of the Andes is a result of thermal thinning of the lithosphere and crustal thickening produced by crustal shortening. Although the model depends upon assumptions about crustal densities and initial conditions, crustal shortening of the order of 100 km is now well established and must certainly be an important component in any model of the central Andes. It would also be hard to argue against a thermal component in the uplift of a plateau that is so extensively covered by volcanics as the Altiplano-Puna. The model can account for the topography without inclusion of magmatic addition to crustal volume.

At the other extreme, a primarily magmatic model for the uplift would require an unusually large rate of extraction of crustal density magmas from the mantle wedge and would imply physiographic characteristics that are not observed. The volcanic material forms a thin cover on a relatively uniformly elevated "tabletop." Although very youthful normal faulting is developed in the northern and southern parts of the plateau, the net deformation is small compared to the much larger late Cenozoic compressional deformations of the crust. There is no evidence for major crustal scale rifts that might result if large amounts of material were injected into the crust as dikes. The physiographic characteristics of the plateau thus indicate that substantial magmatic contributions would have to be in the form of sill-like intrusions or horizontally distributed underplatings of material rather than large vertical dikelike intrusions. The uniform plateau elevation would indicate a rather even distribution of material throughout the large area of the plateau. There is no evidence of topographic bulges that might be expected above large intrusive or underplated volumes concentrated beneath the main volcanic areas along the western side of the plateau.

Instead, the physiography and structure of the Altiplano-Puna reveal a plateaulike uplift bounded on one side by a major thrust belt and on the other by a monoclinal flexure. The topography is a direct expression of the tectonics over much of the plateau because of the low rates of erosion in an arid climate. Thus, in contrast, for example, to the Central Range of Taiwan [*Suppe*, 1981], elevation of the central Andes may be controlled ultimately by lithospheric stresses rather than by denudation.

The model depicts an evolutionary, three-dimensional process rather than steady state, two-dimensional one. Changes in map view shape of the upper plate affect the dip of the slab and vice versa. The three-dimensional aspects of the model presented in this paper imply a very intricate, tightly coupled, and two-way relationship between the configuration of the subducted plate and the plan view outline of the forearc. The following sequence is proposed for the late Cenozoic evolution of the central Andes. An initial seaward concavity in the map view shape of the overriding plate led to an along-strike variation in the dip of the subducted plate, which, by affecting convective processes in the asthenospheric wedge, produced an along-strike variation in width of a thermally weakened zone in the upper plate. The compressional failure of the weakened zone then occurred with an along-strike variation in the amount of shortening and a consequent change in the shape of the leading edge of the overriding plate. The change in shape enhanced, but did not produce, the bending of the Bolivian orocline. The change in shape also involved the Peruvian and Pampean segments moving seaward relative to the central segment, an effect that only partially accounts for the flattening of the subducted plates in the two segments. Effects of subducted plate buoyancy and mantle flow probably also are important.

The model depicted in Figure 7 implies that the changes in dip from relatively steep to nearly flat occur in two regions near 17°S and 23°–27°S. These regions include the anomalous structures and physiographies of the "Abancay Deflection" [*Marocco*, 1978] and the Atacama Basin–Southern Puna, respectively. The location of these regions above along-strike "hinges" in the subducted plate geometry may help to understand the tectonic evolution of these complex regions.

As perhaps the prime example of noncollisional, subduction-related mountain building, the late Cenozoic Andes offer a modern example of processes that may have played a role in the history of more complex mountain belts, such as western North American cordilleras or the Himalayas. The idea that the essential element of cordilleran mountain building in the Andes is compressional failure of a weakened swath of the overriding continental plate, weakened by thermal and magmatic processes operating in the asthenospheric wedge between the plates, is reminiscent of discussions of the Late Creteceous–early Tertiary Laramide-Sevier deformations in the western United States by *Sales* [1968], *Coney* [1972], *Burchfiel and Davis* [1975], and *Armstrong* [1982].

A key feature in explaining the unusual width of the central Andes deformational belt is the low angle of subduction in the central more steeply dipping segment. I hypothesize a 20° dip during the Miocene, while the present dip is about 30°. Two factors may also favor low-angle subduction in addition to the concavity in the shape of the overriding plate. As the East Pacific Rise approaches the subduction zone, (1) the age of the subducted plate decreases and its buoyancy may therefore increase, and (2) the mantle flow beneath the subducted plate may have an increasingly large eastward component. These last two factors would also help explain the postulated low-angle subduction beneath late Mesozoic–early Tertiary western North America.

REFERENCES

Allmendinger, R. W., Tectonic development, southeastern border of the Puna Plateau, northwestern Argentine Andes, *Bull. Geol. Soc. Am., 97*, 1070–1082, 1986.

Allmendinger, R. W., V. A. Ramos, T. E. Jordan, M. Palma, and B. L. Isacks, Paleogeography and Andean structural geometry, northwest Argentina, *Tectonics, 2*, 1–16, 1983.

Allmendinger, R. W., B. L. Isacks, T. E. Jordan, and R. Marrett, Uplift of the Altiplano-Puna plateau: The structural perspective from the SE margin of the Puna, NW Argentina (abstract), *Eos Trans. AGU, 66*, 1088, 1985.

Armstrong, R. L., Cordilleran metamorphic core complexes–from Arizona to southern Canada, *Annu. Rev. Earth Planet. Sci., 10*, 129–154, 1982.

Baker, M. C. W., The nature and distribution of upper Cenozoic ignimbrite centres in the central Andes, *J. Volcanol. Geotherm. Res., 11*, 293–315, 1981.

Baker, M. C. W., and P. W. Francis, Upper Cenozoic volcanism in the central Andes—Ages and volumes, *Earth Planet. Sci. Lett., 41*, 175–187, 1978.

Barazangi, M., and B. L. Isacks, Lateral variations of seismic wave attenuation in the upper mantle above the inclined earthquake zone of the Tonga island arc: Deep anomaly in the upper mantle, *J. Geophys. Res., 76*, 8493–8516, 1971.

Barazangi, M., and B. L. Isacks, Spatial distribution of earthquakes and subduction of the Nazca plate beneath South America, *Geology, 4*, 686–692, 1976.

Barazangi, M., W. Pennington, and B. Isacks, Global study of seismic wave attenuation in the upper mantle behind island arcs using pP waves, *J. Geophys. Res., 80*, 1079–1092, 1975.

Beck, M. E., Jr., R. E. Drake, and R. F. Butler, Paleomagnetism of Cretaceous volcanic rocks from central Chile and implications for the tectonics of the Andes, *Geology, 14*, 132–136, 1986.

Benjamin, M. T., N. M Johnson, and C. W. Naeser, Recent rapid uplift in the Bolivian Andes:
Evidence from fission-track dating, *Geology, 15*, 680–683, 1987.

Bevis, M., and B. L. Isacks, Hypocentral trend surface analysis: Probing the geometry of Benioff zones, *J. Geophys. Res., 89*, 6153–6170, 1984.

Bird, P., Laramide crustal thickening event in the Rocky Mountain foreland and Great Plains, *Tectonics, 3*, 741–758, 1984.

Bowman, I., The physiography of the central Andes, I, The maritime Andes, *Am. J. Sci., 28*, 197–217, 1909a.

Bowman, I., The physiography of the central Andes, II, The eastern Andes, *Am. J. Sci., 28*, 373–402, 1909b.

Bowman, I., *The Andes of Southern Peru*, 336 pp., American Geographical Society, New York, 1916.

Burchfiel, B. C., and G. A. Davis, Nature and controls of Cordilleran orogenesis, western United States: Extension of an earlier synthesis, *Am. J. Sci., 275-A*, 363–396, 1975.

Burchfiel, B. C., P. Molnar, and G. Suaréz, Possible thin-skin tectonics in the eastern Andes of Bolivia and Peru (abstract), *Eos Trans. AGU, 62*, 1047, 1981.

Cande, S., Nazca-South America plate interactions, 80 My to present (abstract), *Eos Trans. AGU, 64*, 865, 1986.

Carey, S. W., The orocline concept in geotectonics, *Proc. R. Soc. Tasmania, 89*, 255–288, 1958.

Chase, C. G., Plate kinematics: The Americas, east Africa, and the rest of the world, *Earth Planet. Sci. Lett., 37*, 355–368, 1978.

Chinn, D. S., and B. L. Isacks, Accurate source depths and focal mechanisms of shallow earthquakes in western South America and in the New Hebrides island arc, *Tectonics, 2*, 529–563, 1983.

Clapperton, C. M., The glaciation of the Andes, *Quat. Sci. Rev., 2*, 83–155, 1983.

Coira, B., J. Davidson, C. Mpodozis, and V. Ramos, Tectonic and magmatic evolution of the Andes of northern Argentina and Chile, *Earth Sci. Rev., 18*, 303–332, 1982.

Coney, P. J., Structural evolution of the Cordillera Huayhuash, Andes of Peru, *Geol. Soc. Am. Bull, 82*, 1863–1884, 1971.

Coney, P. J., Cordilleran tectonics and North America Plate motion, *Am. J. Sci., 272*, 603–628, 1972.

Cross, T. A., and R. H. Pilger, Jr., Controls of subduction geometry, location of magmatic arcs, and tectonics of arc and back-arc regions, *Geol. Soc. Am. Bull., 93*, 545–562, 1982.

Crough, S. T., Apatite fission-track dating of erosion in the eastern Andes, Bolivia, *Earth Planet. Sci. Lett., 64*, 396–397, 1983.

Dalmayrac, B., and P.Molnar, Parallel thrust and normal faulting in Peru and constraints on the state of stress, *Earth Planet. Sci. Lett., 55*, 473–481, 1981.

Dalmayrac, B., G. Laubacher, and R. Marocco, Caractères généraux de l'évolution géologique des Andes Péruviennes, Géologie des Andes Péruviennes, *Trav. Doc. ORSTOM, 122*, Paris, 501 pp., 1980.

Dewey, J. F., Episodicity, sequence and style at convergent plate boundaries, *The Continental Crust and Its Mineral Deposits*, edited by D. W. Strangway, *Special Paper Geol. Assoc. Canada 20*, 553–573, 1980.

Dickinson, W. R., and W. S. Snyder, Plate tectonics of the laramide orogeny, Laramide Folding Associated With Basement Block Faulting in the Western United States, edited by V. Matthews III, *Mem. Geol. Soc. Am., 151*, 355–366, 1978.

Evernden, J. F., S. J. Kriz, and C. Cherroni M., Potassium argon ages of some Bolivian rocks, *Econ. Geol., 72*, 1042–1061, 1977.

Faure, M., and F. Lalavée, Bent structural trends of Japan: Flexural-slip folding related to the Neogene opening of the Sea of Japan, *Geology, 15*, 49–52, 1987.

Fielding, E. J., and T. E. Jordan, Active deformation at the boundary between the Precordillera and Sierras Pampeanas, Argentina, and comparison with ancient Rocky Mountain deformation, *Rocky Mountain Foreland and the Cordilleran Thrust Belt*, edited by W. J. Perry and C. J. Schmidt., *Spec. Pap.Geol. Soc. Amer.* in press, 1988.

Francis, P. W., C. Halls, and M. C. W. Baker, Relationships between mineralization and silicic volcanism in the central Andes, *J. Volcanol. Geotherm. Res., 18*, 165–190, 1983.

Froidevaux, C., and B. L. Isacks, The mechanical state of the lithosphere in the Altiplano-Puna segment of the Andes, *Earth Planet. Sci. Lett., 71*, 305–314, 1984.

Galli-Olivier, C. , Pediplain in northern Chile and the Andean uplift, *Science, 158*, 653–655, 1967.

Grange, F., D. Hatzfeld, P. Cunningham, P. Molnar, S. W. Roecker, G. Suaréz, A. Rodrigues, and L. Ocala, Tectonic implications of the microearthquake seismicity and fault plane solutions in southern Peru, *J. Geophys. Res., 89*, 6139–6152, 1984.

Grant, J. N., C. Halls, W. A. Salinas, and N. J. Snelling, K-Ar ages of igneous rocks and mineralization in part of the Bolivian tin belt, *Econ. Geol., 74*, 838–885, 1979.

Green, A., and B. Wernicke, Possible large-magnitude Neogene extension on the southern Peruvian Altiplano: Implications for the dynamics of mountain building (abstract) *Eos Trans. AGU, 44*, 1241, 1986.

Guest, J. E., Upper Tertiary ignimbrites of the Andean Cordillera of part of the Antofagasta Province, northern Chile, *Geol. Soc. Am. Bull., 80*, 337–362, 1969.

Hager, B. H., and R. J. O'Connell, Subduction zone dip angles and flow driven by plate motion, *Tectonophysics, 50*, 111–133, 1978.

Hasegawa, A., and I. S. Sacks, Subduction of the Nazca plate beneath Peru as determined from seismic observations, *J. Geophys. Res., 86*, 4971–4980, 1981.

Heki, K. Y., Y. Hamano, and M. Kono, Paleomagnetism of the central Andes: A preliminary report, in *Andes Sci. 2*, 67–76, 1983.

Heki, K. Y., Y. Hamano, and M. Kono, Paleomagnetic study of Cretaceous Atajana Formation and the Arica Dike Swarm northernmost Chile, *J. Geomagn. Geoelectr., 37*, 107–117, 1985.

Hirahara, K., and T. Mikumo, Three-dimensional seismic structure of subducted lithospheric plate under the Japan islands, *Phys. Earth Planet. Inter., 21*, 109–119, 1980.

Hollingsworth, S. E., and R. W. R. Rutland, Studies of Andean uplift, part I., Post Cretaceous evolution of the San Bartolo area, northern Chile, *Geol. J., 6*, 49–62, 1968.

Isacks, B. L., Topography and tectonics of the central Andes (abstract), *Eos Trans. AGU, 66*, 375, 1985.

Isacks, B. L., S. M. Kay, E. J. Fielding, and T. Jordan, Andean volcanism: Icing on the cake (abstract), *Eos Trans. AGU, 67*, 1073, 1986.

Jordan, T. E., and R. W. Allmendinger, The Sierras Pampeanas of Argentina: A modern analogue of Laramide deformation, *Am. J. Sci., 286*, 737–764, 1986.

Jordan, T. E., and R. N. Alonso, Cenozoic stratigraphy and basin tectonics of the Andes Mountains, 20°-28° South latitude, *Am. Assoc. Pet. Geol. Bull., 71*, 49–64, 1987.

Jordan, T. E., and M. Gardeweg P., Tectonic evolution of the late Cenozoic central Andes (20°-33°S), in *Cenozoic and Mesozoic Evolution of the Pacific Margin*, edited by Z. Ben-Avraham, Oxford University Press, New York, in press, 1987.

Jordan, T. E., B. L. Isacks, R. W. Allmendinger, J. A. Brewer, V. A. Ramos, and C. J. Ando, Andean tectonics related to geometry of

subducted Nazca plate, *Geol. Soc. Am. Bull., 94*, 341–361, 1983a.

Jordan, T. E., B. L. Isacks, V. A. Ramos, and R. W. Allmendinger, Mountain building in the central Andes, *Episodes, 1983*, 20–26, 1983b.

Kadinski-Cade, K., Seismotectonics of the Chile margin and the 1977 Caucete earthquake of western Argentina, Ph.D. thesis, 253 pp., Cornell Univ., Ithaca, N. Y., 1985.

Karig, D. E., and G. F. Moore, Tectonic complexities in the Bonin island arc system, *Tectonophysics, 27*, 97–118, 1975.

Karig, D. E., R. N. Anderson, and L. D. Bibee, Characteristics of back arc spreading in the Mariana Trough, *J. Geophys. Res., 83*, 1213–1226, 1978.

Kay, S. M., and R. W. Kay, Role of crystal cumulates and the oceanic crust in the formation of the lower crust of the Aleutian arc, *Geology, 13*, 461–464, 1985.

Kay, S. M., V. Maksaev, R. Moscoso, C. Mpodozis, and C. Nasi, Probing the evolving Andean lithosphere: Mid-late Tertiary magmatism in Chile (29°–30.5° S) over the modern zone of subhorizontal subduction, *J. Geophys. Res., 92*, 6173–6190, 1987.

Kelleher, J., and W. McCann, Buoyant zones, great earthquakes, and unstable boundaries of subduction, *J. Geophys. Res., 81*, 4885–4896, 1976.

Kono, M., K. Heki, and Y. Hamano, Paleomagnetic study of the central Andes: Counterclockwise rotation of the Peruvian block, *J. Geodyn., 2*, 193–209, 1985.

Kussmaul, S., P. K. Hörmann, E. Ploskonka, and T. Subieta, Volcanism and structure of southwestern Bolivia, *J. Volcanol. Geotherm. Res., 2*, 73–111, 1977.

Lahsen, A., Upper Cenozoic volcanism and tectonism in the Andes of northern Chile, *Earth Sci. Rev., 18*, 285–302, 1982.

Laubacher, G., Géologie de la cordillère Orientale et de l'altiplano au nord et nord-ouest du Lac Titicaca, *Trav. Doc. ORSTOM, 95*, , 217 pp., 1978.

Lavenu, A., Néotectonique des sédiments Plio-Quaternaires du nord de l'Aliplano Bolivien (Région de La Paz–Ayo-Ayo–Umala), *Cah. ORSTOM, Sér. Géol. 10*(1), 115–126, 1978.

Luyendyk, B. P., Dips of downgoing lithospheric plates beneath island arcs, *Geol. Soc. Am. Bull., 81*, 3411–3416, 1970.

Lyon-Caen, H., P. Molnar, and G. Suárez, Gravity anomalies and flexure of the Brazilian Shield beneath the Bolivian Andes, *Earth Planet. Sci. Lett., 75*, 81–92, 1985.

Marocco, R., Un segment E-W de la chaîne des Andes Péruviennes: La déflexion d'Abancay étude géologique de la Cordillère orientale et des hauts plateaux entre Cuzco et San Miguel sud du Pérou (12°30'S à 14°00'S), *Trav. Doc. ORSTOM, 94*, 195 pp., 1978.

Martinez, C., Structure et évolution de la chaîne Hercynienne et de la Andine dans le nord de la Cordillère des Andes de Bolivie, *Trav. Doc. ORSTOM, 119*, Paris, 352 pp., 1980.

May, S. R., and R. F. Butler, Paleomagnetism of the Puente Piedra formation, central Peru, *Earth Planet. Sci. Lett., 72*, 205–218, 1985.

McBride, S. L., R. C. R. Robertson, A. H. Clark, and E. Farrar, Magmatic and metallogenetic episodes in the northern tin belt, Cordillera Real, Bolivia, *Geol. Rundsch., 72*, 685–713, 1983.

McCabe, R., Implications of paleomagnetic data on the collision related bending of island arcs, *Tectonics, 3*, 409–428, 1984.

McLaughlin, D. H., Geology and physiography of the Peruvian Cordillera, departments of Junin and Lima, *Geol. Soc. Am. Bull., 335*, 591–632, 1924.

Mégard, F., The Andean orogenic period and its major structures in central and northern Peru, *J. Geol. Soc. London, 141*, 893–900, 1984.

Mingramm, A., A. Russo, A. Pozzo, and L. Cazau, Sierras Subandinas, in *Segundo Simposio de Geologia Regional Argentina*, vol. 1, pp. 95–138, Academia Nacional de Ciencias, Cordoba, Argentina, 1979.

Molnar, P., and T. Atwater, Interarc spreading and cordilleran tectonics as alternates related to the age of subducted oceanic lithosphere, *Earth Planet. Sci. Lett., 41*, 330–340, 1978.

Mortimer, C., The Cenozoic history of the southern Atacama Desert, Chile, *J. Geol. Soc. London, 129*, 505–526, 1973.

Mortimer, C., Cenozoic studies in northernmost Chile, *Geol. Rundsch., 2*, 395–420, 1975.

Mortimer, C., Drainage evolution in the Atacama desert of northernmost Chile, *Rev. Geol. Chile, 11*, 3–28, 1981.

Muñoz, J., Chile, Handbook of South American Geology, *Mem. Geol. Soc. Am., 65*, 187–214, 1956.

Newell, N. D., Geology of the Lake Titicaca region, Peru and Bolivia, *Mem. Geol. Soc. Am. 36*, 111 pp., 1949.

Noble, D. C., and E. H. McKee, Spatial distribution of earthquakes and

subduction of the Nazca plate beneath South America: Comment, *Geology, 5, 576–578*, 1977.

Nur, A., and Z. Ben-Avraham, Volcanic gaps and the consumption of aseismic ridges in South America, Nazca Plate: Crustal Formation and Andean Convergence, edited by L. D. Kulm, *Mem. Geol. Soc. Am., 154*, 729–740, 1981.

Palmer, H. C., A. Hayatsu, and W. D. MacDonald, Paleomagnetic and K-Ar age studies of a 6 km-thick Cretaceous section from the Chilean Andes, *Geophys. J. R. Astron. Soc., 62*, 133–153, 1980a.

Palmer, H. C., A. Hayatsu, and W. D. MacDonald, The Middle Jurassic Camaraca Formation, Arica, Chile: Paleomagnetism, K-Ar age dating and tectonic implications, *Geophys. J. R. Astron. Soc., 62*, 155–172, 1980b.

Pardo-Casas, F., and P. Molnar, Relative motion of the Nazca (Farallon) and South American plates since Late Cretaceous time, *Tectonics, 6*, 233–248, 1987.

Pilger, R. H., Jr., Plate reconstructions, aseismic ridges and low-angle subduction beneath the Andes, *Geol. Soc. Am. Bull., 92*, 448–456, 1981.

Pilger, R. H., Cenozoic plate kinematics, subduction and magmatism: South American Andes, *J. Geol. Soc. London, 141*, 793–802, 1984.

Prince, R. A., W. Schweller, W. Colbourn, G. Shepherd, G. Ness, and A. Masias, Part I, Bathymetry of the Peru-Chile continental margin and trench, *Geol. Soc. Am. Map Chart Ser., MC–34*, 1980.

Ramos, V. A., El Mesozoico de la Alta Cordillera de Mendoza: Reconstruccion tectonica de sus facies–Argentina, *Actas, IV Chile Congreso Geologico Chileno*, vol. 2, 104–118, Universidad del Norte Chile, Antofagasta, Chile, 1985.

Rutland, R. W. R., J. E. Guest, and R. L. Grasty, Isotopic ages and Andean uplift, *Nature, 208*, 677–678, 1965.

Sales, J. K., Crustal mechanics of cordilleran foreland deformation: A regional and scale-model approach, *Am. Assoc. Petr. Geol. Bull., 52*, 2016–2044, 1968.

Schwab, K., Ein beitrag zur jungen Bruchtektonik der Argentinischen Puna and ihr Verhaltnis zu den angrenzenden Andenabschnitten, *Geol. Rundsch. 59*, 1064–1087, 1970.

Schwab, K., Die stratigraphie in der Umgebung des Salar de Cauchari (N.W. Argentinien), *Geotekton. Forsch. 43*, 166 pp., 1973.

Schweller, W. J., L. D. Kulm, and R. A. Prince, Tectonics, structure and sedimentary framework of the Peru-Chile trench, Nazca Plate: Crustal Formation and Andean Convergence, edited by L. D. Kulm, *Mem. Geol. Soc. Am., 154*, 323–349, 1981.

Sclater, J. G., B. Parsons, and C. Jaupart, Oceans and continents: Similarities and differences in the mechanisms of heat loss, *J. Geophys. Res., 86*, 11,535–11,552, 1981.

Sébrier, M., J. L. Mercier, F. Mégard, G. Laubacher, and E. Carey-Gailhardis, Quaternary normal and reverse faulting and the state of stress in the central Andes of south Peru, *Tectonics, 4*, 739–780, 1985.

Segerstrom, K., Matureland of northern Chile and its relationship to ore deposits, *Geol. Soc. Am. Bull., 74*, 513–518, 1963.

Sheffels, B., B. C. Burchfiel, and P. Molnar, Deformational style and crustal shortening in the Bolivian Andes (abstract), *Eos Trans. AGU, 44*, 1241, 1986.

Stewart, J. W., Neogene peralkaline igneous activity in eastern Peru, *Geol. Soc. Am. Bull., 82*, 2307–2312, 1971.

Strecker, M. R., R. Alonso, F. Rivelli, and R. Mon, Quaternary tectonic movements in the Argentine Puna, 24° to 27° S latitude, *Geol. Soc. Am. Abstr. Programs, 17*, 729, 1985.

Suárez, G., P. Molnar, and B. C. Burchfiel, Seismicity, fault plane solutions, depth of faulting, and active tectonics of the Andes of Peru, Ecuador, and southern Colombia, *J. Geophys. Res., 88*, 10,403–10,429, 1983.

Suppe, J., Mechanics of mountain building and metamorphism in Taiwan, *Mem. Geol. Soc. China, 4*, 67–89, 1981.

Thomas N. A., Beitrag zur tektonik nord Chiles, *Geol. Rundsch., 59*, 1013–1027, 1970.

Thorpe, R. S., P. W. Francis, and R. S. Harmon, Andean andesites and crustal growth, *Philos. Trans. R. Soc. London, Ser. A, 301*, 305–320, 1981.

Tosdal, R. M., A. H. Clark, and E. Farrar, Cenozoic polyphase landscape and tectonic evolution of the Cordillera Occidental, southernmost Peru, *Geol. Soc. Am. Bull. , 95*, 1318–1332, 1984.

Tovish, A., G. Schubert, and B. P. Luyendyk, Mantle flow pressure and the angle of subduction: Non-Newtonian corner flows, *J. Geophys. Res., 83*, 5892–5898, 1978.

Turcotte, D. L., and D. C. McAdoo, Geoid anomalies and the thickness of

the lithosphere, *J. Geophys. Res., 84*, 2381–2387, 1979.

Turner, J. C. M., Estratigrafía de la Sierra de Santa Victoria y adyacencias, *Bol. Acad. Nac. Cienc. Argent., 41*, 163–196, 1960.

Turner, J. C. M., Estratigrafía del Nevado de Cachi y sector al oeste (Salta), *Acta Geol. Lilloana, 3*, 191–226, 1961.

Turner, J. C. M., Perfil transversal de la Puna, latitud 22° 15' S approximada, *Actas Segundas Jornadas Geol. Argent., 3*, 355–378, 1966.

Turner, J. C. M., Un perfil transversal de la Puna Austral, latitud 26° S. República Argentina, *Asoc. Geol. Argent. Rev., 24*, 361–366, 1969.

Turner, P., H. Clemmey, and S. Flint, Paleomagnetic studies of a Cretaceous molasse sequence in the central Andes (Coloso formation, northern Chile), *J. Geol. Soc. London, 141*, 869–876, 1984.

Utsu, T., Seismological evidence for anomalous structure of island arcs with special reference to the Japanese Region, *Rev. Geophys., 9*, 839–890, 1971.

Uyeda, S., and H. Kanamori, Back arc opening and the mode of subduction, *J. Geophys. Res., 84*, 1049–1061, 1979.

Valencio, D. A., J. F. Vilas, and I. G. Pacca, The significance of the paleomagnetism of Jurassic-Cretaceous rocks from South America: Predrift movements, hairpins and magnetostratigraphy, *Geophys. J. R. Astron. Soc., 73*, 135–151, 1983.

Vicente, J. C., F. Sequeiros, M. A. Valdivia, and J. Zavala, El sobre-escurrimiento de Chincha-Lluta: Elemento del accidente mayor andino al NW de Arequipa, *Bol. Soc. Geol. Peru, 61*, 77 – 100, 1979.

Wilson, J. T., and K. Burke, Two types of mountain building, *Nature, 239*, 448–449, 1972.

Wollard, G. P., Regional isostatic relationships in the U.S., *The Earth Beneath the Continents, Geophys. Monogr. Ser.*, vol. 10, edited by J. S. Steinhart and T. J. Smith, pp. 557–594, AGU, Washington, D. C., 1966.

Wortel, M. J. R., Spatial and temporal variations in the Andean subduction zone, *J. Geol. Soc. London, 141*, 783–791, 1984.

Wortel, M. J. R., and N. J. Vlaar, Age-dependent subduction of oceanic lithosphere beneath South America, *Phys. Earth Planet. Inter., 17*, 201–208, 1978.

Yamaoka, K., and Y. Fukao, Spherical shell tectonics: Effects of sphericity and inextensibility on the geometry of the descending lithosphere, *J. Geophys. Res., 24*, 27–53, 1986.

Yamaoka, K., and Y. Fukao, Why do island arcs form cusps at their junctions?, *Geology, 15*, 34–36, 1987.

Yuen, D. A., L. Fleitout, G. Schubert, and C. Froidevaux, Shear deformation zones along major transform faults and subducting slabs, *Geophys. J. R. Astron. Soc., 54*, 93–119, 1978.

Zhao, W.-L., and W. J. Morgan, Uplift of the Tibetan Plateau, *Tectonics, 4*, 359–369, 1985.

B. L. Isacks, INSTOC Cornell Andes Project, Department of Geological Sciences, Snee Hall, Cornell University, Ithaca, NY 14853.